We are IntechOpen, the world's leading publisher of Open Access books Built by scientists, for scientists

4,800
Open access books available

122,000
International authors and editors

135M
Downloads

Our authors are among the

154
Countries delivered to

TOP 1%
most cited scientists

12.2%
Contributors from top 500 universities

CLARIVATE ANALYTICS BOOK CITATION INDEX INDEXED

WEB OF SCIENCE™

Selection of our books indexed in the Book Citation Index in Web of Science™ Core Collection (BKCI)

Interested in publishing with us?
Contact book.department@intechopen.com

Numbers displayed above are based on latest data collected.
For more information visit www.intechopen.com

2

Electropolymerization of Some Ortho-Substituted Phenol Derivatives on Pt-Electrode from Aqueous Acidic Solution; Kinetics, Mechanism, Electrochemical Studies and Characterization of the Polymer Obtained

S.M. Sayyah*, A.B. Khaliel, R.E. Azooz and F. Mohamed
Polymer Research Laboratory, Chemistry Department, Faculty of Science, Beni-Suef University 62514, Beni-Suef City, Egypt

1. Introduction

One of the promising methods for waste water remediation is The electrochemical oxidation of hazardous organic species [Fleszar & Jolanta, *1985;* Comninellis, 1994]. Phenols due to their slow degradation, bioaccumulation and toxicity constitute a large group of organic pollutants. The quantitation of phenolic compounds in environmental, industrial and food samples is currently of great interest, which can be found in soils and groundwater [Wang et al., 1998]. Also, these compounds are important synthesis intermediates in chemical industry such as resins, preservatives, pesticides, etc. Another, the main sources of phenolic waste are in glass fiber insulation manufacture on petroleum refineries. Phenol and substituted phenolic compounds such as catechol, chlorophenol are hydroquinones and discharged in the effluent from a number of chemical process industries. Today, these compounds are found in relatively high amount in domestic and industrial wastewater, discharged mainly from the mechanical industries. Many treatment technologies are in use or have been proposed for phenol recovery or destruction.

The electrooxidation of phenolic compounds can be occurs as follows: in the first step of electrooxidation of phenols, phenoxy radicals are generated, then these species can be either oxidized further or be coupled, forming ether and oligomeric or polymeric compounds [Wang et al ,1991; Iotov, & Kalcheva, 1998]. Electropolymerization of phenol beings with the formation of the phenoxy radical, or it can react with a molecule of phenol to give predominantly a para-linked dimeric radical. This radical may be further oxidized to form a neutral dimmer or it may attach another molecule. The dimer may be further oxidized create oligomers to polymers. Formation of the insoluble polyphenol results in deactivation of electrode surface. The relative rates of the two pathways (polymerization and forming quinonic structure) depend on the phenols concentration, the nature of electrode, pH, solvent, additives, electrode potential and current density [Gattrell & Kirk,1993]. Electropolymerization of phenols occur on different electrodes, such as Fe, Cu, Ni, Ti, Au, Pt

and other type of electrodes [Iotov, & Kalcheva, 1998; Ezerskis & Jusys, 2002]. Deactivation of electrode due to the phenol polymerization is more characteristic in alkaline medium. Insoluble high molecular weight species block the electrode surface and prevent effective electrooxidation of phenol.

In the present work, we seek to contrast the electro-oxidation of OCP and OHP from aqueous H_2SO_4 medium as electrolyte using cyclic voltammetry technique. The kinetic study of the oxidation processes will be useful for optimize the parameters control it. Mechanisms of the electrochemical polymerization will be discussed using electrochemical data. Also, the characterization of the obtained polymer films were carried out by elemental analysis, TGA, SEM, XRD, IR, UV-vis., ^{1}H-NMR spectroscopy. We hope to have films with good characters to be used in applications (i.e. dye removal and pH sensor).

2. Expermental

2.1 Materials

OCP was obtained from Hopkin & Williams (Dagenham, Essex, UK), Sulfuric acid, K_2HPO_4, KHphthalate, Borax, NaOH, Hydrochloric acid and $NaHCO_3$ were provided by Merck (Darmstadt, Germany). OHP and MB dye was provided by Aldrich. All chemicals are of analytical pure grade and used as received. All solutions were prepared by using freshly double-distilled water

2.2 Electropolymerization cell

Electropolymerization of the monomers and formation of the polymer films was carried out using potentiodynamic technique. The cell used is shown in Fig. (1). This cell is made from transparent Prespex trough, which has the inside dimensions of 8cm length, 2.5cm width and 3cm height.

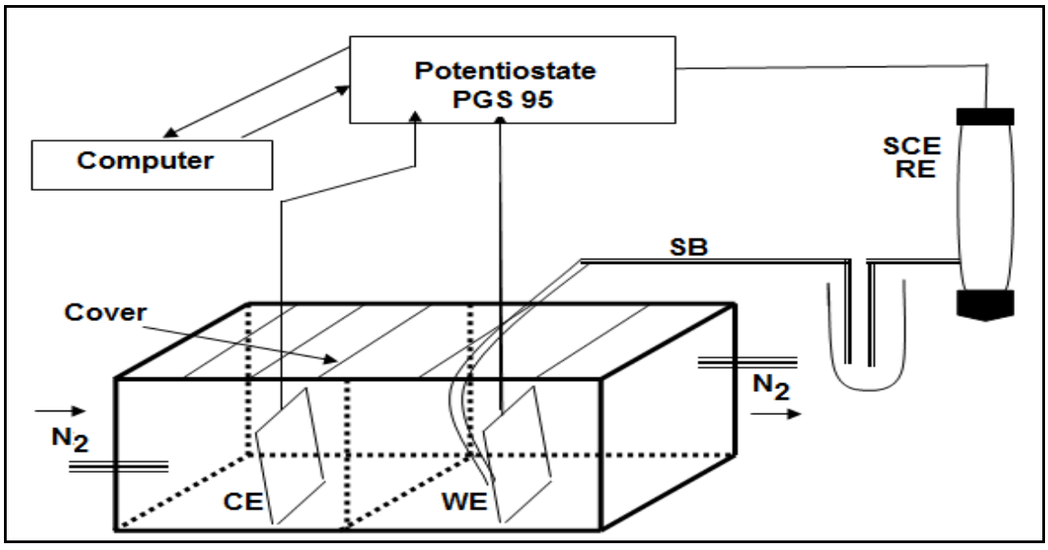

Fig. 1. Three electrode cell used for electropolymerization and cyclic voltammetry measurements. Were CE is counter electrode, WE is working electrode, SB is salt bridge, SCE is the standard calomel electrode and RE is the reference electrode.

2.2.1 Electrodes

2.2.1.1 Working electrode

The working electrode (WE) was a platinum sheet with dimensions of 1cm length and 0.5 cm width

2.2.1.2 Auxiliary electrode

The auxiliary (counter) electrode (CE) was a platinum foil with the same dimensions as the WE. Before each run, both the WE and the CE were cleaned and washed thoroughly with water, double distilled water, rinsed with ethanol and dried.

2.2.1.3 Reference electrode

A saturated calomel electrode (SCE) was used as a reference electrode. The values of the electrode potential in the present work are given relative to this electrode. The potential value for the SCE is 0.242 V vs. NHE at 25 ^{o}C. SCE was periodically calibrated and checked.
Electrochemical experiments were performed using the Potentiostat / Galvanostat Wenking PGS 95. i-E curves were recorded by computer software from the same company (Model ECT). Except otherwise stated, the potential was swept linearly from starting potential into the positive direction up to a certain anodic potential with a given scan rate and then reversed with the same scan rate up to the starting cathodic potential.
For each run, freshly prepared solutions as well as a cleaned set of electrodes were used. All experiments were conducted at a given temperature (± 0.5 ^{o}C) with the help of circular water thermostat. After polymer film formation, the working electrode was withdrawn from the cell, rinsed thoroughly with a doubly distilled water to remove any traces of the formed constituents in the reaction medium. The deposited polymer film was subjected to different experimental tests to characterize it.

2.2.2 Procedure

Potentiodynamic cyclic voltammetry measurements during the formation of the polymer films on the surface of the working electrode was carried out in the electrochemical cell shown in Fig.(1).The cell was filled with the test solution (aqueous solution containing H_2SO_4 as supporting electrolyte, and monomer). The working and counter electrodes were introduced in the cell. The reference electrode was attached to the cell by U-shaped salt bridge (SB) ended with a fine capillary tip (Luggin –Harber probe)wherein the reference electrode was positioned very closed to the working electrode to minimize the over potential due to electrolyte resistance .The bridge was filled with the test solution. Before and during measurements a current of pure nitrogen gas was bubbled in the test solution to remove dissolved oxygen.
Electrochemical experiments were performed using the potentiostat / Galvanostat Wenking PGS 95. i-E curves were recorded by computer software from the company (Model ECT).
Except otherwise stated ,the potential was swept linearly from the starting potential vs. (SCE) into the positive direction up to a certain anodic potential with a given scan rate and then reversed with the same scan rate up to the starting cathodic potential.
For each run, freshly prepared solutions as well as a cleaned set of electrodes were used. All experiments were conducted at a given temperature (± 0.5 ^{o}C) with the help of circular water thermostat. After polymer film formation, the working electrode was withdrawn from the cell, rinsed thoroughly with doubly distilled water to remove any traces of the medium

constituents. The deposited polymer film was subjected to different experimental tests to characterize it.

2.3 Characterization of the electro-prepared polymers

2.3.1 UV-vis, IR and ^{1}H-NMR spectroscopy, TGA and elemental analysis

UV-vis. absorption spectra of the prepared polymer sample was measured using Shimadzu UV spectrophotometer (M160 PC) at room temperature in the range 200-400 nm using dimethylformamide (DMF) as a solvent and reference. IR measurements were carried out using shimadzu FTIR-340 Jasco spectrophotometer (Japan) by KBr pellets disk technique. ^{1}H-NMR measurements were carried out using a Varian EM 360 L, 60-MHz NMR spectrometer. NMR signals of the electropolymerized sample were recorded in dimethylsulphoxide (DMSO) using tetramethylsilane as internal standard. TGA of the obtained polymer was performed using a Shimadzu DT-30 thermal analyzer (Shimadzu, Kyoto, Japan). The weight loss was measured from ambient temperature up to 600 ^{o}C, at the rate of 20 ^{o}C min^{-1} and nitrogen 50cc min^{-1} to determine the degradation rate of the polymer. Elemental analysis was carried out in the micro-analytical center at Cairo University (Cairo, Egypt) by oxygen flask combustion and dosimat E415 titrator (Metrohm).

2.3.2 Scanning electron microscopy and X-ray diffraction

Scanning electron microscopic (SEM) analysis was carried out on the as-prepared polymer film deposited on Pt-working electrode surface using a JSM-T20 Electron Probe Microanalyzer (JEOL, Tokyo, Japan). The X-ray diffraction analysis (XRD) (Philips 1976 Model 1390, Netherlands) was operated under the following conditions that were kept constant for all the analysis processes: X-ray tube, Cu; scan speed, 8 deg min^{-1}; current, 30 mA; voltage, 40 kV; preset time, 10 s.

2.4 Determination of the kinetic rate law of the electropolymerization reaction

The amount of polymer electrodeposited on the electrode surface can be determined directly from the peak current density (i_p) [Sayah et al, 2010] therefore, The peak current density (i_p) is proportional to the electropolymerization rate ($R_{P,E}$) at a given concentration of the monomer and H_2SO_4. The kinetic equation was calculated from the value of anodic peak current density (i_p) measured at each concentration during the electroformation of polymer. In this case, we used the value of (i_p) instead of ($R_{P,E}$). Therefore, the kinetic rate law can be expressed as follows

$$R_{P,E} = i_p = k_E [\text{Acid}]^a [\text{Monomer}]^b \quad (1)$$

where a and b are the reaction orders with respect to acid and monomer concentrations respectively, and k_E is the kinetic rate constant calculated from the electrochemical measurements.

2.5 Potentiometric data and pH measurements

The electropolymerization were performed with a three-electrode system mention above in section. Using a potential range -0.2 ~ +0.9V (vs.SCE) with a scan rate of 25 mVs^{-1}. Finally, a POCP modified Pt-electrode was ready for further experiments. the thickness of the polymer films were controlled by varying the no of repetitive cycles from 3 to 15 cycles as the thickness of polymer films were positively correlated with the no of repetitive cycles.

Potentiometric data were recorded by using (two electrodes system) shown in Fig.(2). Where the working electrode is the prepared POCP modified Pt-electrode with different thickness and the reference electrode is SCE. The potential of system (the electrode and the tested buffer solution) were recorded after immersion for 5 minute by using Avometer DT3900, then the polymer electrode removed from the solution and rinsed with bidistilled water before immersing in anther buffer solution for the next measurement All pH measurements were performed using the modified electrode as the pH sensor and SCE is the reference electrode. The actual pH of solution was determined by pH meter (HANNA Instruments pH 211).

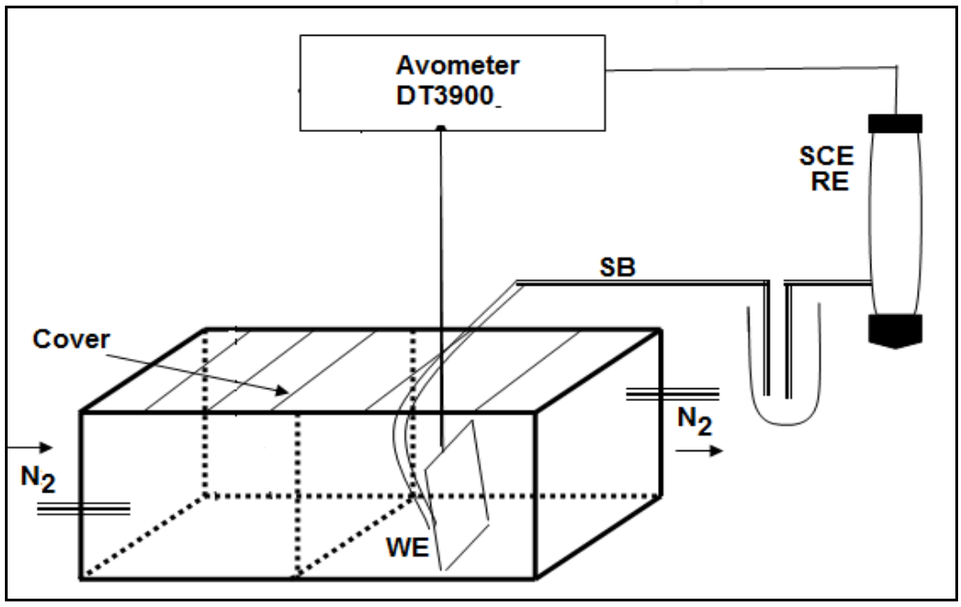

Fig. 2. Two electrode cell used foe potentiometric measurements.

2.6 Adsorption of methylene blue (MB) dye

Different concentrations of MB solution was added to 0.05gm of POHP previously deposited potentiodynamically on Pt electrode surface in 50 ml measuring flask and with continuous stirring for 2 h and then filtration. The concentration of dye in the filtrate was determined at different time intervals by using UV-Vis spectrophotometer at 664 nm for MB dye, the equilibrium uptake was calculated according to the following equation:

$$Q_e = (C_o - C_e)\, V / W \quad (2)$$

Where Qe is the amount adsorbed at equilibrium, C_o is the initial concentration of dye, C_e is the equilibrium conc. of the dye solution, V is volume of solution (L) and W is the mass of polymer taken for the experiment (mg)

The percentage removal of dye was calculated as

$$\text{Percentage removal} = 100\,(C_o - C_e) / C_o \quad (3)$$

3. Results and discussion

3.1 Electropolymerization kinetics and mechanisms of of OCP and OHP

3.1.1 Electropolymerization

Electropolymerization of OCP or OHP on platinum electrode from aqueous solution containing 0.6M H_2SO_4 at 303 K in the absence and presence of monomer, was studied by cyclic voltammetry at potential between -366 and +1780 mV(vs. SCE) with scan rate of 25 mVs^{-1}.

The obtained voltammograms in absence and presence of monomer is represented in Fig. 1(a-c). The voltammogram in the absence of monomer exhibit an oxidation peak (I) which developed at -300 mV vs. SCE, which is a result of hydrogen adsorption on Pt electrode [Arslan et al, 2005]. While, the voltammograms in the presence of OCP exhibit two oxidation peaks (I and II) that progressively developed at -300 and +863 mV (vs. SCE) repetitively and one reduction peak (II') at +248 mV (vs. SCE). While in the presence of OHP ; two oxidation peaks (I and II) that progressively developed at --200 and +622 mV (vs. SCE) repetitively and one reduction peak (II') at +0.20 mV (vs. SCE). One one hand, the first oxidation peaks (I) are a result of hydrogen reduction [Arslan et al, 2005] as mentioned above where, the second oxidation peaks (II) correspond to oxidation of monomer to give phenoxy radical which adsorbed on Pt-electrode [Gattrell & Kirk,1993]. The adsorbed radicals react with

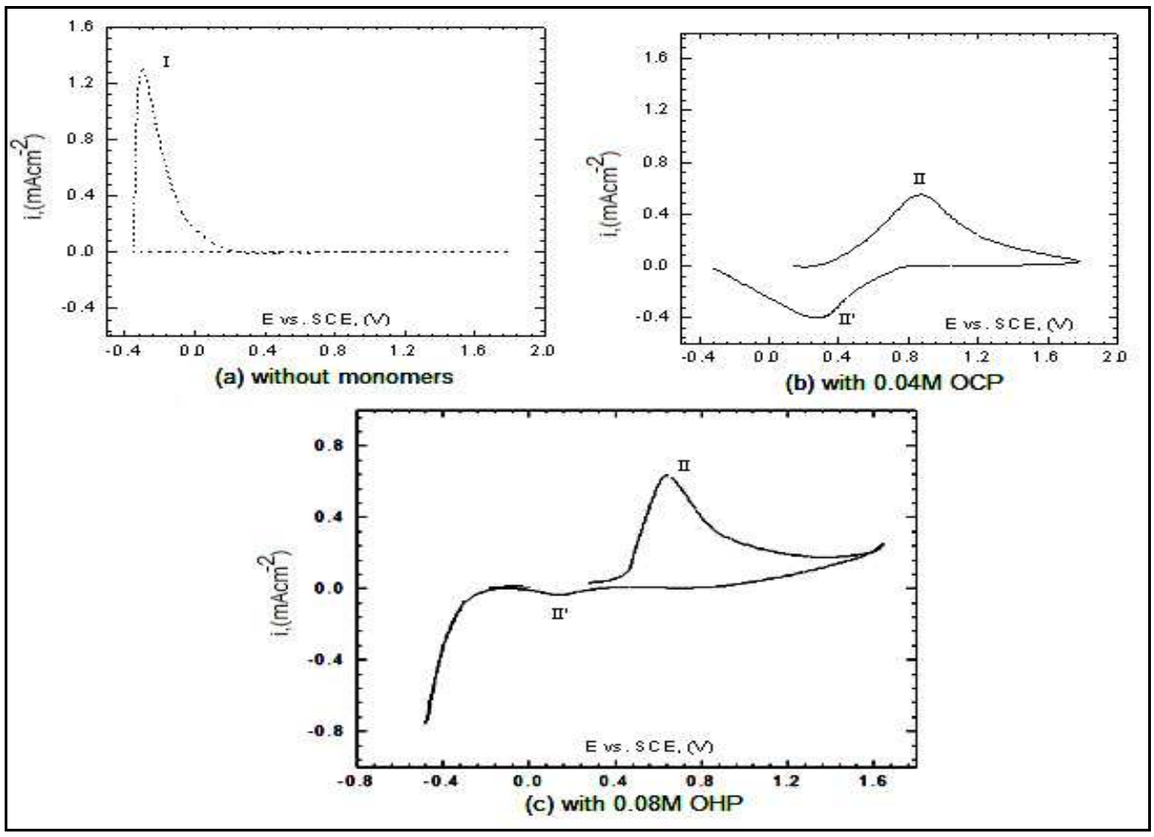

Note: peak (I) in both (b) and (c) is not shown in the figure.

Fig. 3. Cyclic voltammograms of solutions containing 0.06M H_2SO_4 at 303 K with scan rate 25mVs^{-1}.

other monomer molecule via head-to-tail coupling to form predominantly a para-linked dimeric radical and so on to form oligomer and polymer film; this film is a chain of isolated aromatic rings (polyethers) without π-electrons delocalization between each unit as shown in schemes (1 and 2). The oxidation occurs at more positive values ~ + 863 and +622 mV vs. SEC where the presence of (Cl and OH) make the oxidation process difficult.

On reversing the potential scan from, the reversing anodic current is very small indicating the presence of polymer layer adhered to the Pt-surface [Sayyah et al, 2010]. One cathodic peak (II') was found which could be ascribed to the reduction of the formed polymer films.

The effects of repetitive cycling on Pt- electrode in aqueous solution containing 0.6M H_2SO_4 with and without monomer at 303 K are shown in Fig. 4 (a-c). The data reveal that, in absence of monomer, the repetitive cycling show the oxidation peak (I) only. The current of this peak (i_{pI}) is almost the same and not affected with cycling up to 6 cycles (c.f. fig. 4 (a)).

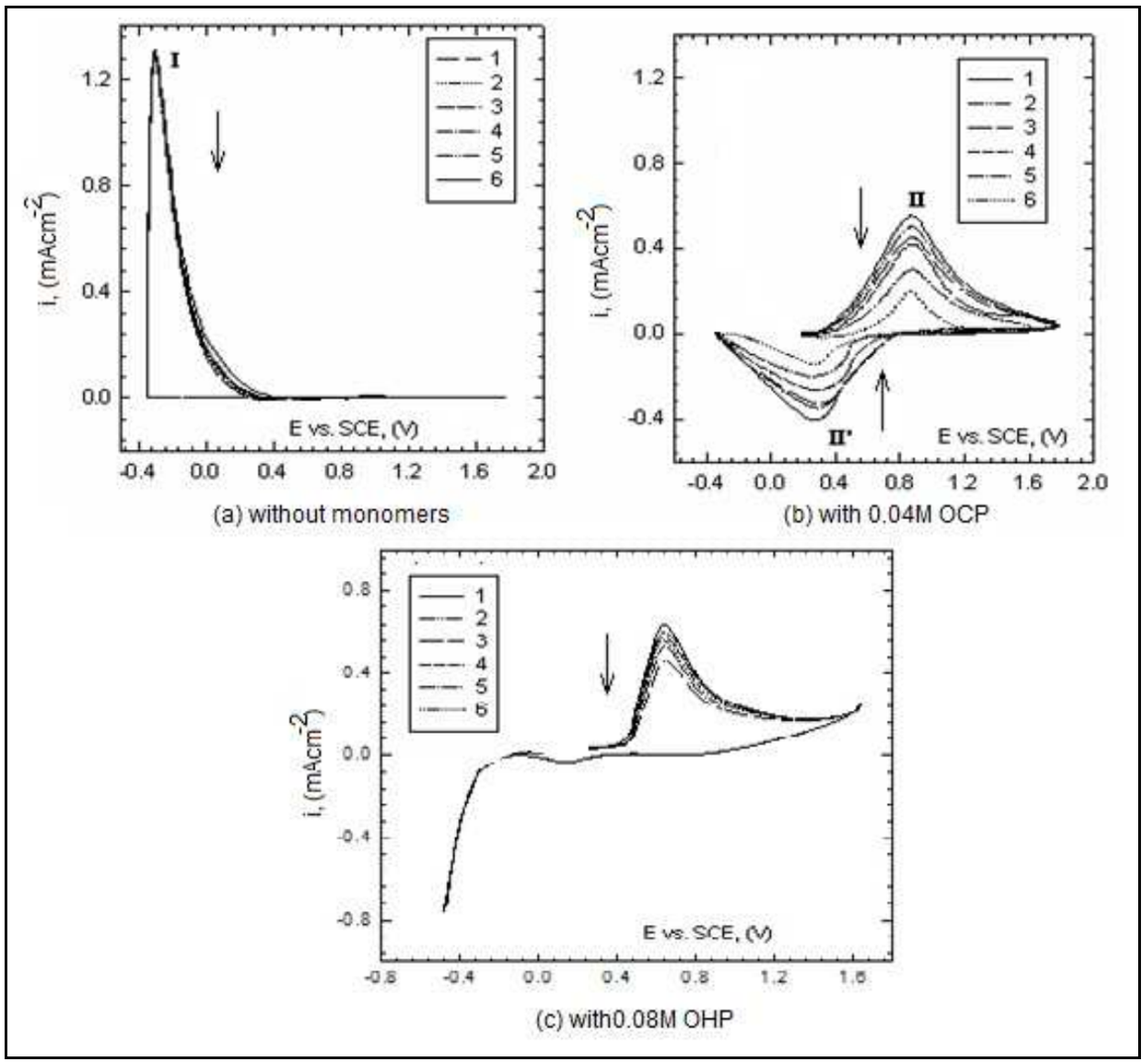

Fig. 4. Repetitive cycling of electropolymerization from solution containing 0.6M H_2SO_4 at 303 K with scan rate 25 mVs^{-1}

This means that, surface area of electrode is not affected by the H_2 adsorption where, in presence of monomers (OCP or OHP) the data reveal that, during the second cycle both the oxidation and the reduction peak currents decrease significantly with repetitive cycling. This behavior is observed elsewhere as a result of fouling of electrode [Arslan et al, 2005] where phenolic products block the electrode surface and the formed film hinders diffusion of further phenoxide ions to the electrode surface, thereby causing a significant decrease in the anodic peak current and also decrease the cathodic peak current. The potential position of the redox peaks does not shift with increasing number of cycles, indicating that the oxidation and the reduction reactions are independent on the polymer thickness [Sayyah et al, 2010].
Figure 5 (a and b) illustrates the influence of the scan rate (15 – 45 mV s^{-1}) on the potentiodynamic anodic polarization curves for OCP and OHP from aqueous solution containing 0.6 M H_2SO_4 at 303 K on platinum electrode. It is obvious that both the anodic and cathodic peak current densities (i_{pII} and $i_{pII'}$) in the two cases increases with the increasing of the scan rate. This behavior may be explained as follows, when an enough potential is applied at Pt- surface causing oxidation of species in solution, a current arises due to the depletion of the species in the vicinity of the Pt- surface. As a consequence, a concentration gradient appears in the solution. The current (i_p) is proportional to the gradient slope, dc/dx, imposed (i = dc/dx). As the scan rate increase the gradient increase and consequently the current (i_p).

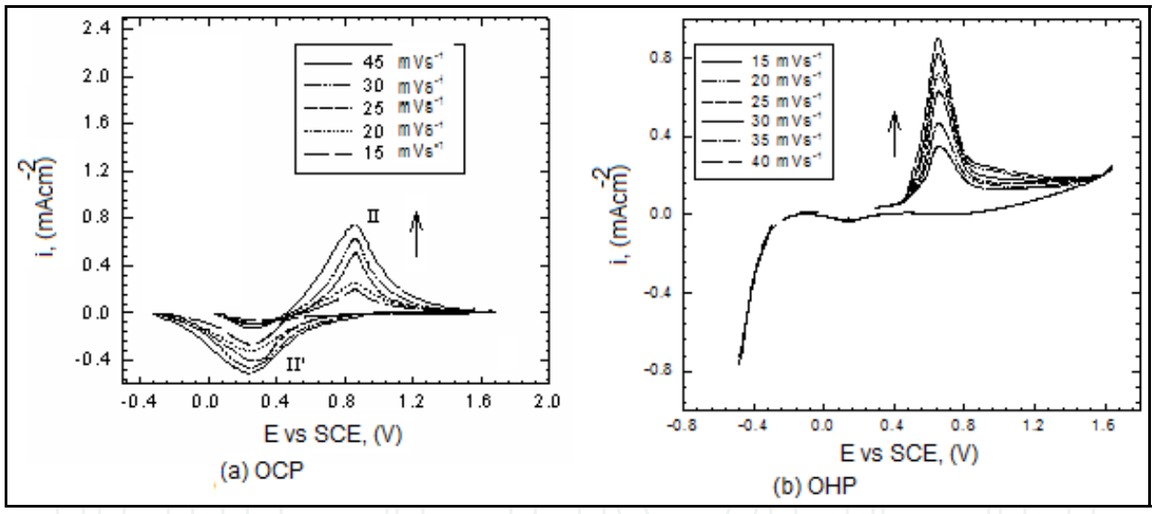

Fig. 5. Effect of Scan rate on electropolymerization on Pt electrode from solution containing 0.6M H_2SO_4 at 303 K.

Figure 6 (a and b) shows the linear dependency of the anodic peak current densities (i_{pII}) - which is corresponding to the formation of the polymer films POCP and POHP repetitively- versus the square root of scan rate ($v^{1/2}$). This linear relation suggests that the oxidation of OCP to POCP and/or OHP to POHP may be described by a partially diffusion-controlled process (diffusion of reacting species to the polymer film / solution interface) where the correlation coefficients (r^2) is higher than 0.9 but not equal to 1.0 suggesting the non-ideal simulation relation (i.e: the process is not completely diffusion control but it is exactly a partially diffusion control. Values of i_p are proportional directly to $v^{1/2}$ according to Randless [Randless, 1984] and Sevick [Sevick, 1948] equation:

$$i_{pII} = 0.4463\ n\ F\ A\ C\ (\ n\ F\ v\ D\ /\ R\ T\ )^{1/2} \quad (4)$$

where n is the number of exchanged electron in the mechanism, F is Faraday's constant (96485 $Cmol^{-1}$), A is the electrode area (cm^2), C is the bulk concentration, D is the analyst diffusing coefficient (cm^2s^{-1}), and v is the scan rate (Vs^{-1}). R is the universal gas constant (8.134 $Jmol^{-1}K^{-1}$), T is the absolute temperature (K).The calculated values of D (at 0.6 M H_2SO_4 at 303 K with scan rate from 15 to 45 mV s^{-1}) are shown in Table 1;

Scan rate, (Vs^{-1})	Diffusing coefficient, (m^2s^{-1})	
	OCP→POCP	OHP→POHP
0.015	1.83676 x 10^{-11}	4.41282 x 10^{-11}
0.020	2.15245 x 10^{-11}	8.26886 x 10^{-11}
0.025	7.16612 x 10^{-11}	1.09351 x 10^{-10}
0.030	9.11262 x 10^{-11}	1.15739 x 10^{-10}
0.045	1.07765 x 10^{-10}	1.59405 x 10^{-10}

Table 1. Calculated values of Diffusion coefficients.

The values of D are seen to be constant for both cases over the range of sweep rates, which again shows that the oxidation process is diffusion-controlled [sayyah et al, 2010].
Figure 6 (a and b) shows the linear dependence of the anodic current peak, (i_{pII}) versus $v^{1/2}$. These linear regression equations are;
For OCP; i_{pII} *(mA) = 0.207* $v^{1/2}$ *(mV* $s^{-1})^{1/2}$ *– 0.60 :* r^2*=0.90 and,*
For OHP; i_{pII} *(mA) = 0.228* $v^{1/2}$ *(mV* $s^{-1})^{1/2}$ *– 0.53:* r^2*=0.99*
From Fig. 6 and the above equations we notice that; 0.9 < correlation coefficient (r^2) <1. So we suggest that the electroformation of both POCP and POHP may be described partially by a diffusion-controlled process (diffusion of reacting species to the polymer film/solution interface). [Ardakani et al, 2009] It seems that, initially the electroformation of radical cations

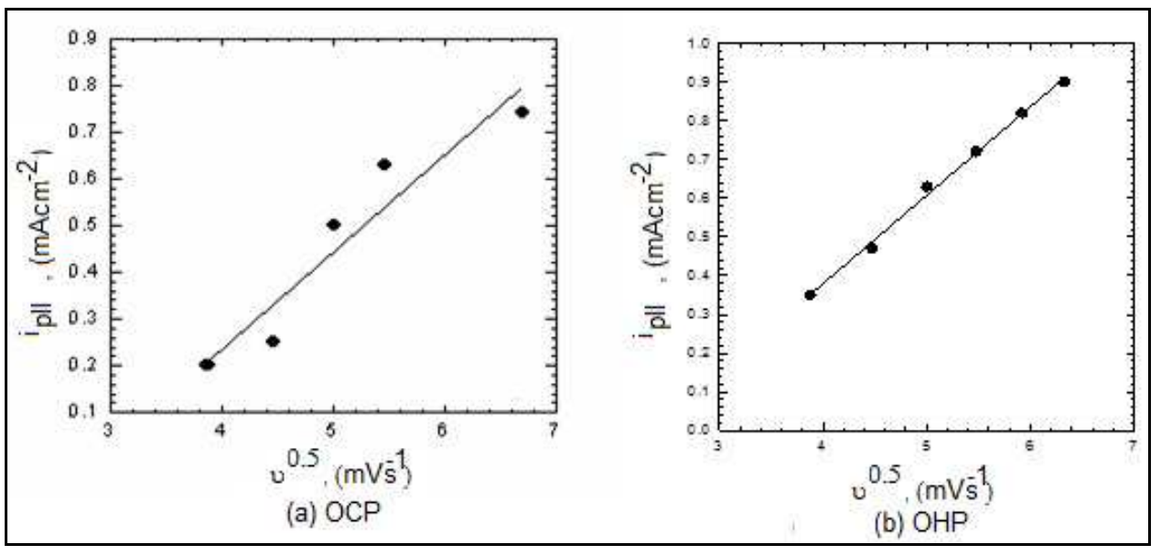

Fig. 6. Relation between ipII and square root of scan rate $\upsilon^{0.5}$

is controlled by charge transfer process. When the polymers become thick, the diffusion of reactant inside the film becomes the slowest step, the process changed to diffusion transfer, which confirms the data in Figure 4.
The intercepts in Figure 6 are small and negative, -0.60 and -0.53 for OCP and OHP respectively, which could be attributed to a decrease of the active area of the working electrode during the positive scan [Zanartu et al , 2002] or the increase of the covered area of working electrode by the adhered polymer sample, which confirm the data of Figure 4 .

3.1.2 Kinetic studies

The electropolymerization kinetics was investigated by using aqueous solution containing (different monomer concentrations in the range between 0.01 and 0.04M in case of OCP and in the range between 0.3 and 0.6M in case of OHP where H_2SO_4 concentration in the range between 0.3 and 0.6M at 303 K in both case. The cyclic voltammogram for each monomeric systems and the relation between the log i_{pII} vs log [monomer] or log i_{p11} vs log [H_2SO_4] are plotted from which linear relations were obtained.

3.1.2.1 Effect of monomer concentration on the electropolymerization processes

The influence of OCP and OHP concentrations on the CV behavior was studied using scan rate of 25 mVs^{-1} is shown in Figure7 (a and b). The voltammograms show that, the anodic peak current densities (i_{pI1}) increase with the increasing of the monomer concentration. This is obvious due to the increased availability of the electroactive species, OCP and OHP in solution, which is again in accordance with Eq.(4).
At higher monomer concentrations (i.e. concentration > 0.04 M for OCP and concentration > 0.08 M for OHP), no noticeable increase in peak currents was observed. This suggests that, at higher concentration, the oxidation reaction is not limited by diffusion alone
A double logarithmic plot of the current density related to oxidation peaks (II) against monomers concentrations are graphically represented in Figure 7 (c and d). Straight lines with slope of 1.1 for OCP and 0.96in case of OHP were obtained. Therefore, the reactions order with respect to both monomers concentration is a first-order reaction.

3.1.2.2 Effect of H2SO4 concentration on the polymerization process

The influence of acid concentration in the range between (0.3 and 0.6M) on the CV using of OCP or OHP using scan rate of 25 mVs^{-1} is represents in Figure 8 (a and b). Voltammograms show that, the anodic peak current densities (i_{pI1}) increase with the increasing of the acid concentration in both cases. At higher acid concentrations for both cases (i.e. concentration > 0.6 M), no noticeable increase in peak currents were observed but, it began to decrease as a result of degradation and the solubility of the polymer film from the platinum surface. A double logarithmic plot of the current density related to oxidation peaks (II) against acid concentrations in the range between 0.3 and 0.6M is graphically represented in Figure8 (c and d). Straight lines with slope of 0.98 in case of OHP and of 0.74in case of OHP were obtained. Therefore, the reactions may be considered as first-order with respect to H_2SO_4 concentration in both cases. Depending upon the above results, the kinetic rate laws obtained from this method can be written as:
For OCP; $R_{P,E} = k_E\,[monomer]^{1.1}\,[acid]^{0.98}$ *and*
For OHP; $R_{P,E} = k_E\,[monomer]^{0.96}\,[acid]^{0.74}$
Where, $R_{P,E}$ is the electropolymerization rate and k_E is the kinetic rate constant.

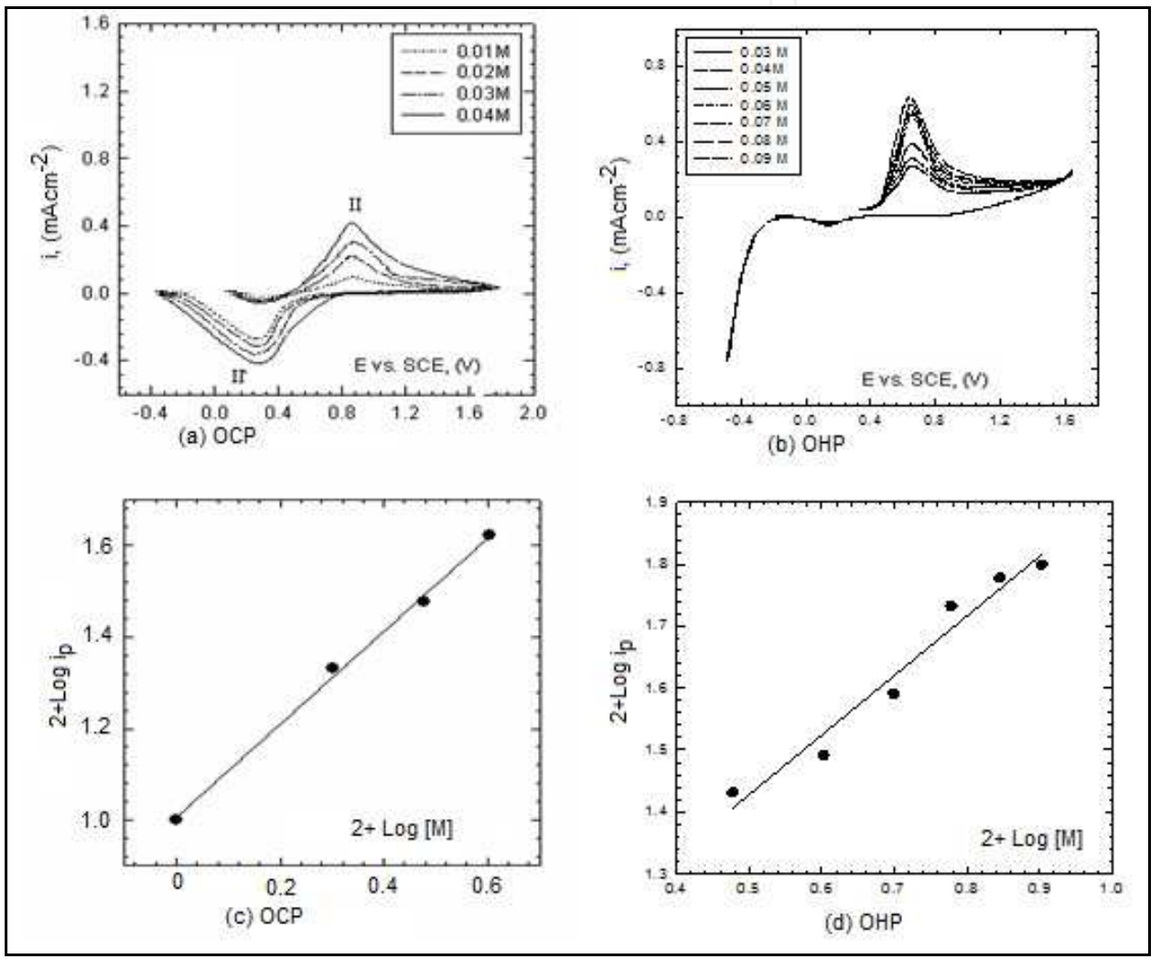

Fig. 7. Cyclic voltammetry curves showing the effect of monomers concentration on electropolymerization and its related double logarithmic plot.

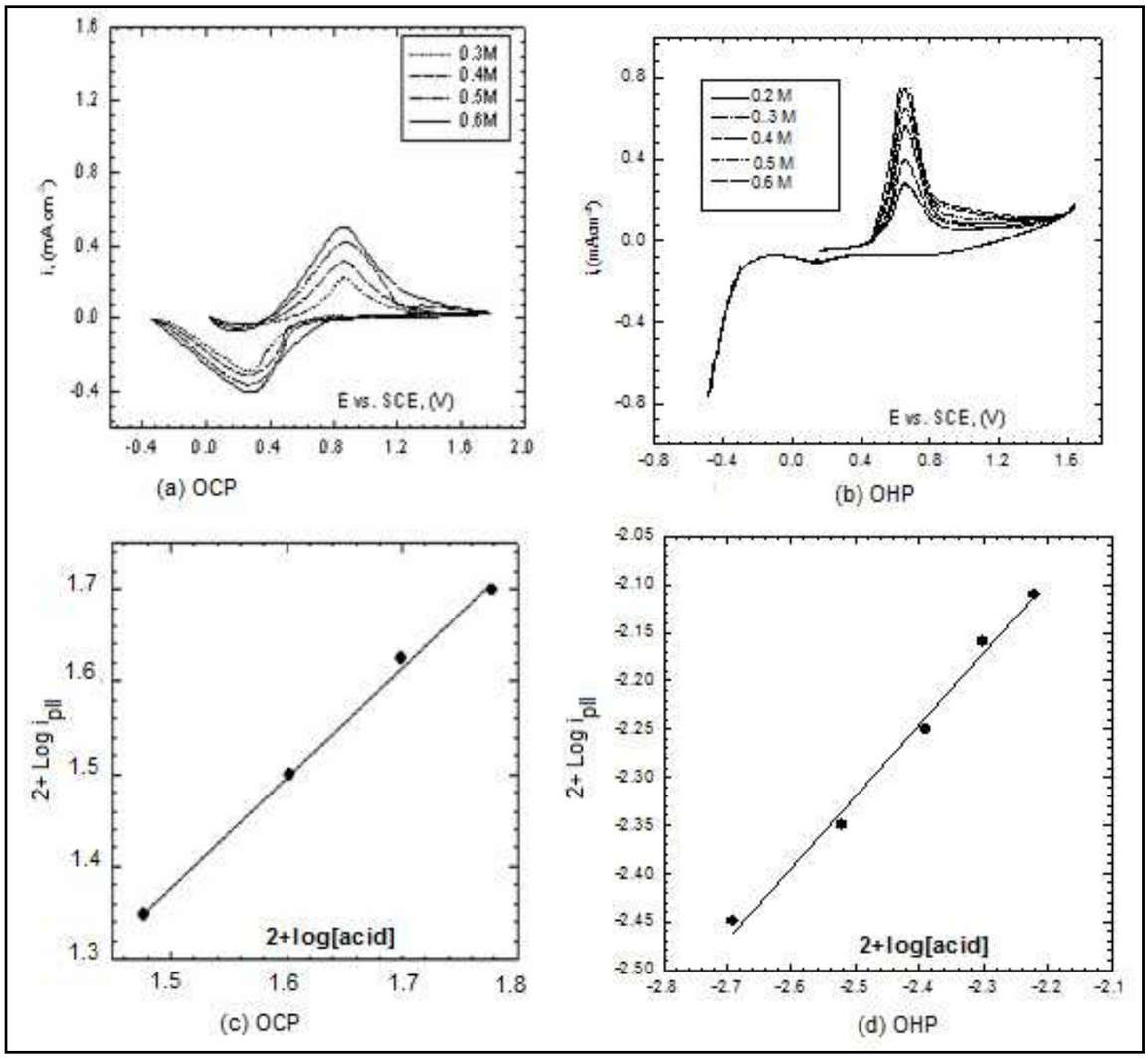

Fig. 8. Cyclic voltammetry curves showing the effect of acid concentration on electropolymerization and its related double logarithmic plot.

3.1.2.3 Effect of temperature and calculation of thermodynamic parameters

The potentiodynamic polarization curves as a function of the solution temperature in the range between 293 and 313 K under the optimum experimental conditions as mentioned above (i.e. 0.04M monomer and 0.6M acid in case of OCP or 0.08M monomer and 0.6M acid in case of OHP) were illustrated in Figure 9(a and b). From the figure, it is clear that, an increase of the reaction temperature resulted in a progressive increase of the charge included in the anodic peaks. The plot of the log (i_{p1}) versus 1/T is represented in Figure 9 (c and d), straight lines are obtained with slopes equal to -1.44 in case of OCP and -1.17 in case of OHP. The apparent activation energies were calculated using Arrhenius equation [sayyah et al, 2010] and it is found to be 27.57kJ mol^{-1} for OCP and 22.39 kJ mol^{-1} for OHP. The enthalpy ΔH^* and entropy ΔS^* of activation for the electropolymerization reaction can be calculated from Eyring equation plot at different temperatures (Fig. 9(e and f)) we obtained linear relationships with slopes of $-\Delta H^*/2.303R$ and intercepts of log {(R/Nh) +

$\Delta S^*/2.303R$}. From slopes and intercepts the values of ΔH^* and ΔS^* were found to be 31.54 k J mol^{-1} and -99.68 JK^{-1} mol^{-1}, respectively for OCP and 19.87k J mol^{-1} and –286.69 JK^{-1} mol^{-1}, respectively for OHP.

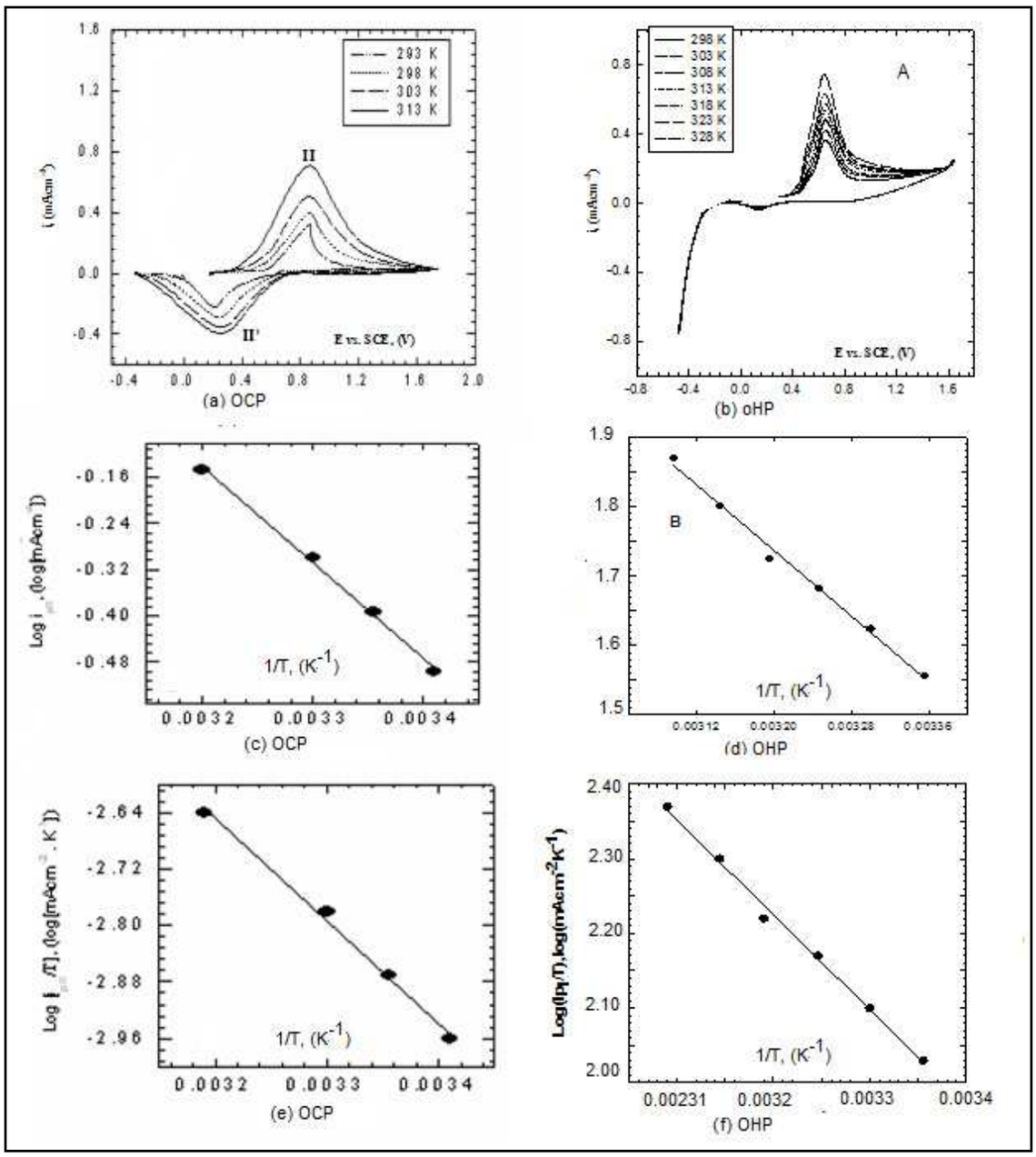

Fig. 9. Cyclic voltammetry curves for the effect of temperature on the electropolymerization, Arrhenius plot and Eyring equation plot

3.2 Electroactivity of the Pt-polymer film

The obtained polymer films adhere Pt-electrode -after preparation at the optimum conditions of preparation (0.04M monomer and 0.6M Acid for OCP and 0.08M monomer

and 0.6M Acid for OHP at 303 K using 25 mV s^{-1})- were transferred to another cell with only 0.6M H_2SO_4 and cycled in the same range as the above work. The obtained date shows that, the oxidation peaks that was developed at +863 SCE and +622 mV vs. SCE for OCP and OHP respectively were disappear completely but the H_2 peak (developed at -300 and -200 mV vs. SCE for OCP and OHP respectively) are still found and a broad reduction peaks is observed (at ~ 300 and 200mV vs. SCE for OCP and OHP respectively) which is attributed to the reduction of the formed polymer films. The lack of oxidation peaks confirm the insulating properties of the films and lake of active species inside the polymer films. By repetitive cycling, the current of peak I still the same where the current of peak II decreases as a result of decreasing the polymer amount on Pt surface.

3.3 Mechanisms of electropolymerization

The anodic oxidative polymerization of OCP is preceded in different steps as follows:

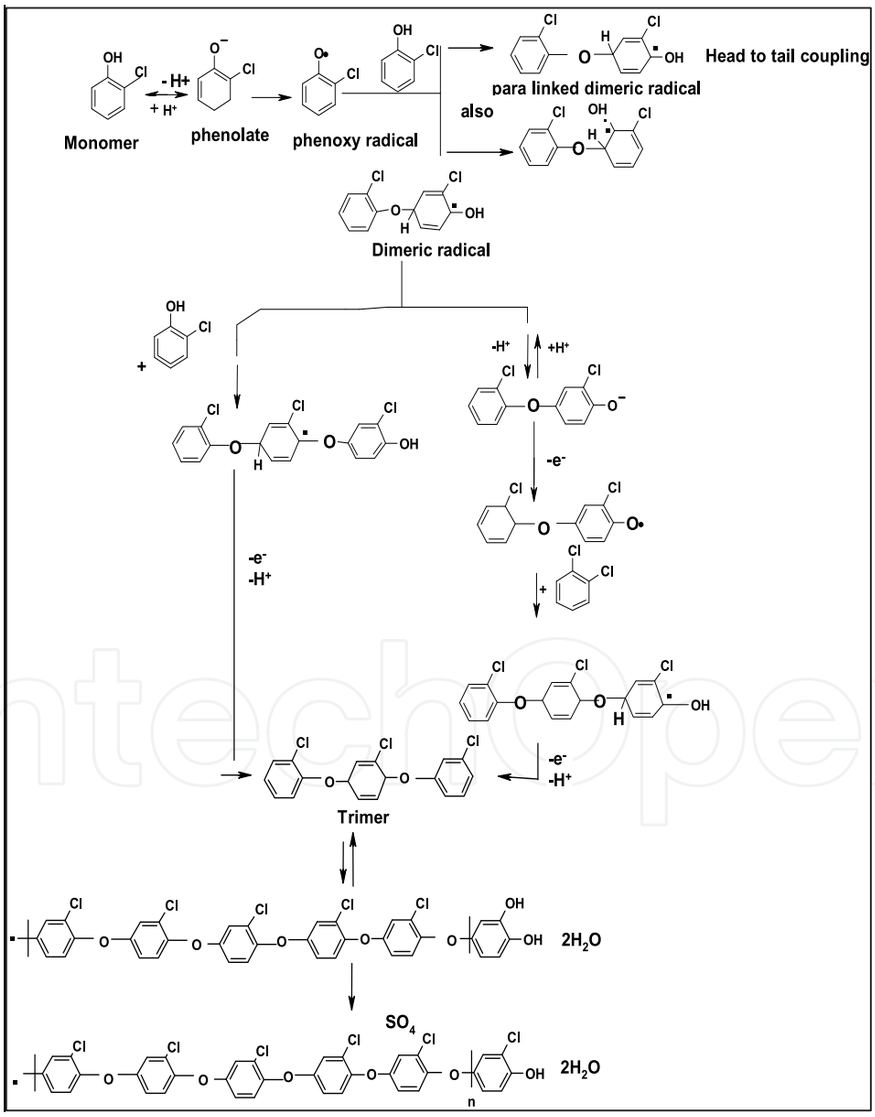

Scheme 1. The mechanism of electropolymerization of OCP.

The anodic oxidative polymerization of OHP is preceded in different steps as follows;

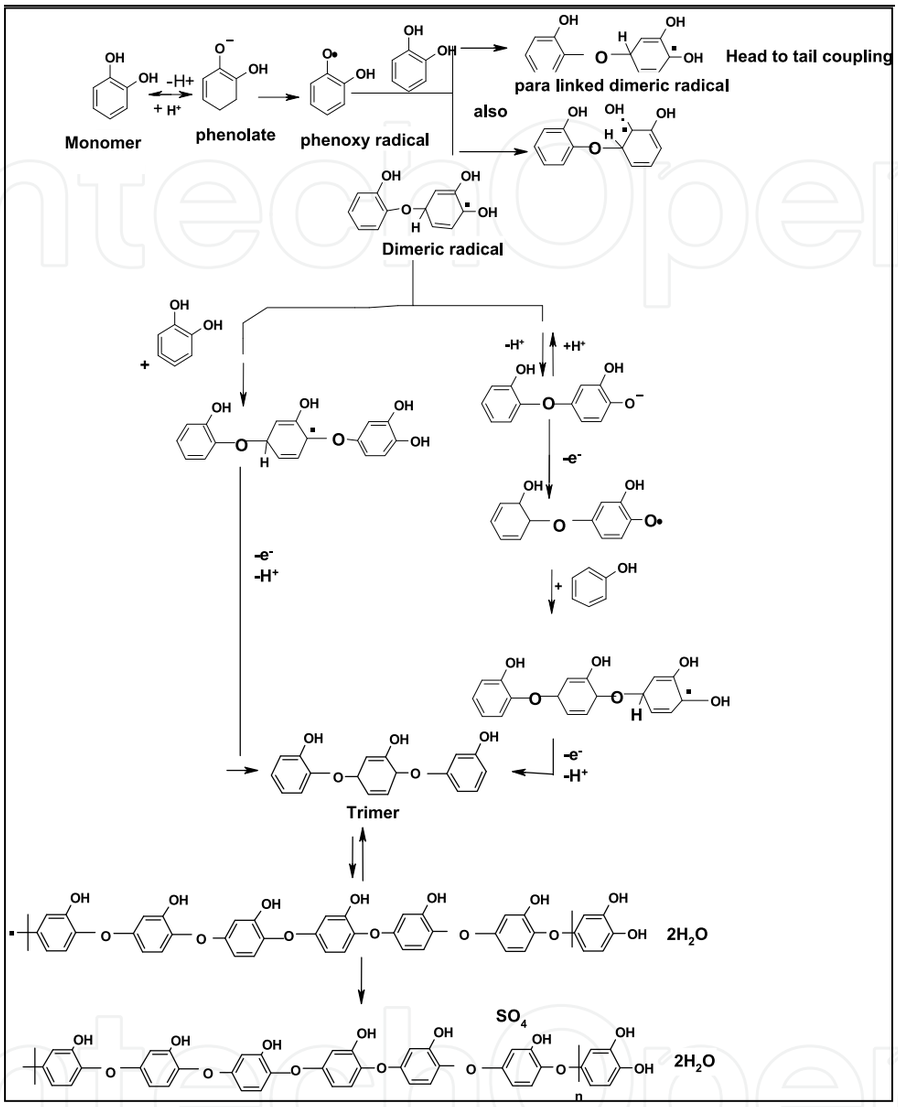

Scheme 2. The mechanism of electropolymerization of OHP.

3.4 Structure determination of the obtained polymers by elemental and spectroscopic an

3.4.1 Elemental analysis

Elemental analysis of the obtained polymers by anodic oxidative Electropolymerization of OCP and OHP were carried out in the micro- analytical laboratory at Cairo University. The percentage C, H, Cl and S for all investigated polymers samples are summarized in Table 2

The found elemental analyses are in a good agreement with the calculated data for the above suggested structures in schemes 1and 2.

No	Structure of polymer	Elemental analysis			
		C%	H%	Cl%	S%
		Cal/found	Cal/found	Cal/found	Cal/found
1	POCP	47.1 47.5	2.48 2.10	23.22 23.01	4.18 4.20
2	POHP	55.24 54.25	3.83 4.15	-- --	4.00 3.48

Table 2. Elemental analytical data of the prepared homopolymers

3.4.2 Spectroscopic analysis

3.4.2.1 Ultraviolet spectroscopic studies

The UV vis. spectra of OCP and its homopolymer POCP and OHP and its homopolymer POHP are shown in Fig 10 (a-d)

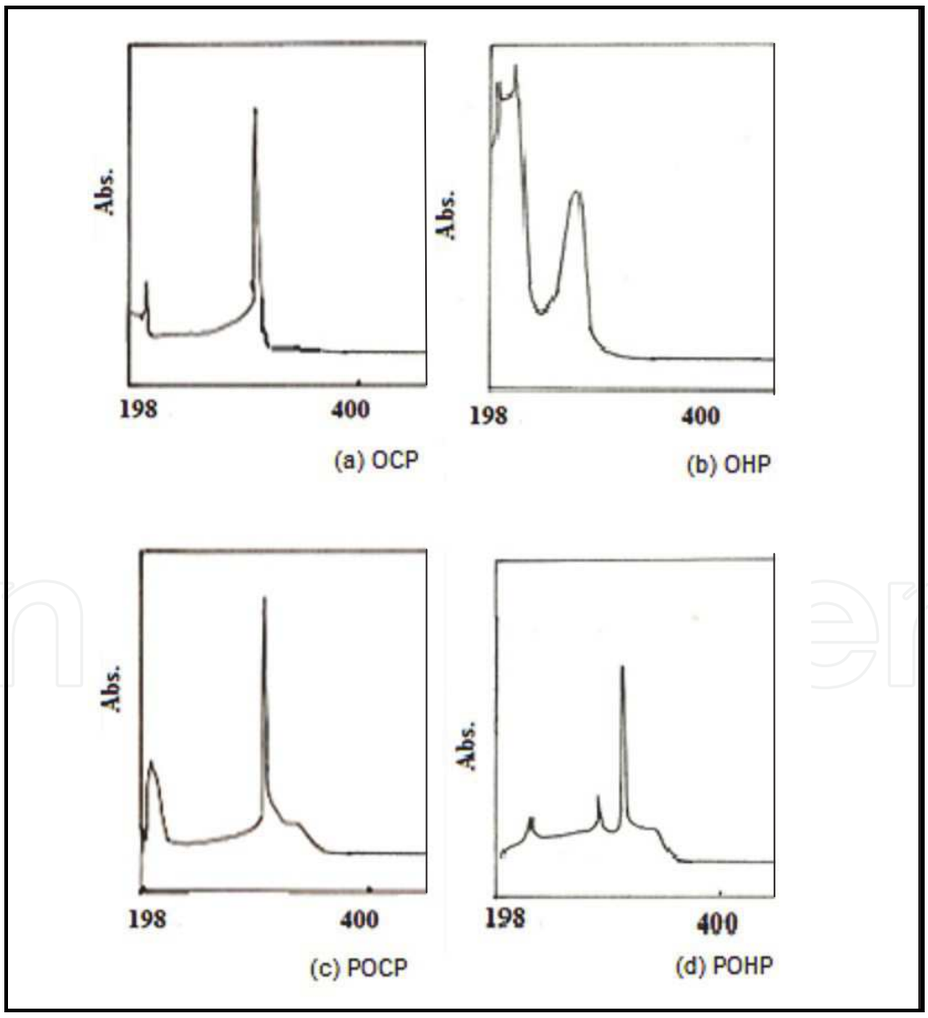

Fig. 10. Uv-vis. Spectra of OCP, OHP, POCP and POHP.

The absorption bands shown in the spectra are summarized in Table 3.

λ_{max}				Assignment
OCP	POCP	OHP	POHP	
---	---	200	---	π- π* transition
212	208	---	---	
---	---	225	223	
---	---	---	---	
---	---	---	---	
---	---	---	273	
306	307	302	305	

Table 3. The Uv-vis. assignments.

3.4.2.2 Infrared spectroscopic studies

The infrared spectra of OCP monomer and its prepared homopolymer POCP are represented in Fig. 11(a) where the infrared spectra of OHP monomer and its prepared homopolymer POHP are represented in Fig. 11(b). The IR absorption bands and their assignments are given in Tables 4 and 5.

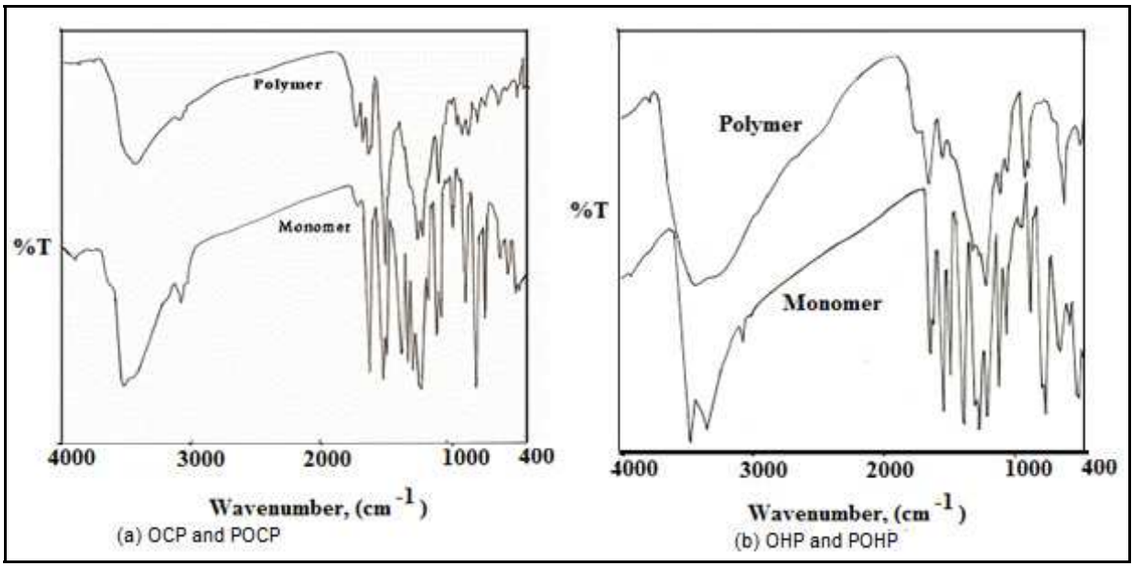

Fig. 11. IR spectra of OCP, POCP, OHP and POHP.

Wave number(cm^{-1})		Assignments
Name		
OCP	POCP	
750^{s}	--	CH out of plane bending for 1,2 di-substituted benzene ring
833^{s}	--	
--	823^{s}	CH out of plane bending for 1,2,4 tri-substituted benzene ring
925^{s}	920^{m}	Stretching vibration for C-Cl group
1028^{s}	1058^{s}	Stretching vibration for C-O group
1055^{s}		
--	1187^{m}	Stretching for incorporation in the polymer sulphate group
1456^{s}	--	Stretching vibration of C=C in benzene ring
1482 ^{s}	1475^{s}	
1589^{s}	1490^{s}	
1645^{m}	1698^{s}	
3073^{m}	3070^{w}	Stretching vibration for CH aromatic
3520^{b}	3419^{b}	Stretching vibration intermolecular hydrogen solvated OH group or end group OH of polymeric chain

Table 4. IR adsorption bands and their assignments for OCP and POCP.(*where; s: strong, w: weak, b: broad, m:medium*}

Wave number(cm^{-1})		Assignments
Name		
OHP	POHP	
746^{s}	--	CH out of plane bending for 1,2 di-substituted benzene ring
762^{m}	--	
851^{s}	--	
--	857^{s}	CH out of plane bending for 1,2,4 tri-substituted benzene ring
--	1176.4^{m}	SO_4 incorporation in the polymer
1188^{s}	1197^{s}	C-O stretching vibration
1268^{s}	1251^{s}	
1468^{s}	1475.3^{s}	C=C stretching vibration in benzene ring
--	1508^{s}	
1597^{s}	--	
1619^{s}	--	
--	1642^{s}	
3049^{w}	3100^{w}	CH stretching vibration in benzene ring
--	3382^{b}	intermolecular hydrogen solvated OH stretching vibration
3451^{m}	3743^{b}	Free OH stretching vibration
3328^{m}		

Table 5. IR adsorption bands and their assignments for OHP and POHP.(*where; s: strong, w: weak, b: broad, m:medium*)

3.4.2.3 ^{1}HNMR spectroscopic studies

The ^{1}HNMR spectrum of the prepared POCP and POHP are represented in Fig.12 (a and b). The figure shows two solvent signals at δ=2.55 ppm and δ=3.55 ppm in case of POCP where in case of POHP the solvent signals appear at δ=2.15 ppm and δ=2.55 ppm. The protons of benzene rings in the polymeric structures appear in the region from δ=6.04 to δ=8 ppm in both cases. The singlet signal appears at δ=4.3 ppm in case of POCP and at 5.5 ppm in case of POHP is attributed to OH protons for water of solvation. The singlet signal appears at δ=10.1ppm in case of POCP and at δ=9.5 is attributed to OH proton attached to for benzene ring. The signals of different (OH) are disappeared when deuterated water was added to the investigated sample.

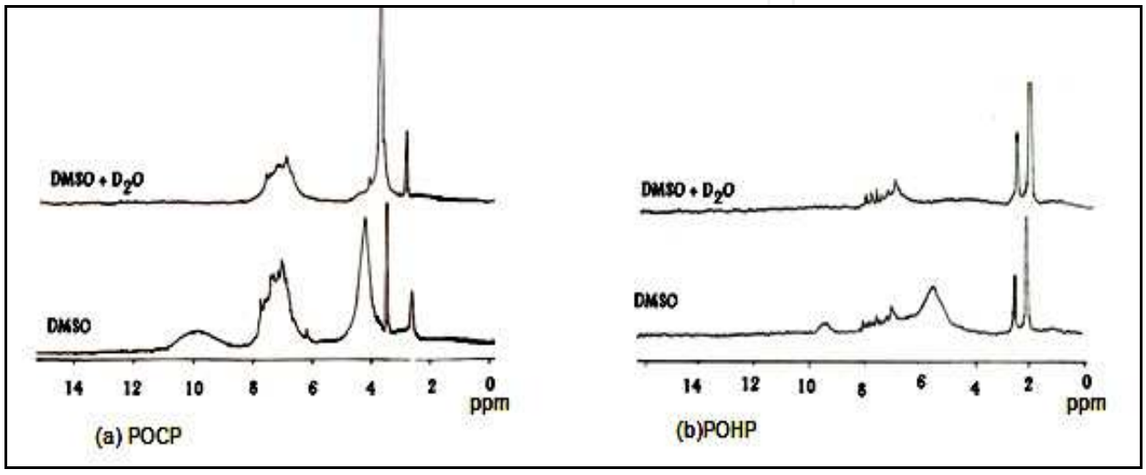

Fig. 12. ^{1}HNMR spectra of POCP and POHP in DMSO and DMSO+D_2O.

3.4.2.4 Thermogravimetric analysis(TGA)

Thermogravimetric analysis (TGA) for the electrochemically prepared POCP and POHP samples have been investigated and the TGA-curve is represented in Figure 13 (a and b).

The TGA steps of the prepared POCP are shown in Fig 13(a) from which it is shown that there are three stages during thermolysis of the POCP sample

The first stage : including the loss of $2H_2O$ molecules in the temperature range between 25^{o}C and 120^{o}C , The weight loss was found to be (5.30%) which is in good agreement with the calculated value (5.70%)this is in good agreement with what was found in the literature for water release [Sayyah et al 2010].

second stage: includes the loss of the dopant species , SO_3 and one benzenoide ring in the temperature range between 120 ^{o}C and 400^{o}C , the weight loss for this step was found to be 24.04% which is in good agreement with the calculated value (24.8%)

The third stage: in the range of temperature >490 ^{o}C, the remaining part of the polymer decomposition,is equal to 70.70. The found data equal to 69.5.

The TGA steps of the prepared POHP are shown in Fig. 13 (b) from which it is shown that there are four stages during thermolysis of the polymer sample

The first stage: including the loss of $2H_2O$ molecules in the temperature range between 25 ^{o}C and 100^{o}C , The weight loss was found to be(4.35%) which is in good agreement with the calculated value(4.6%) .

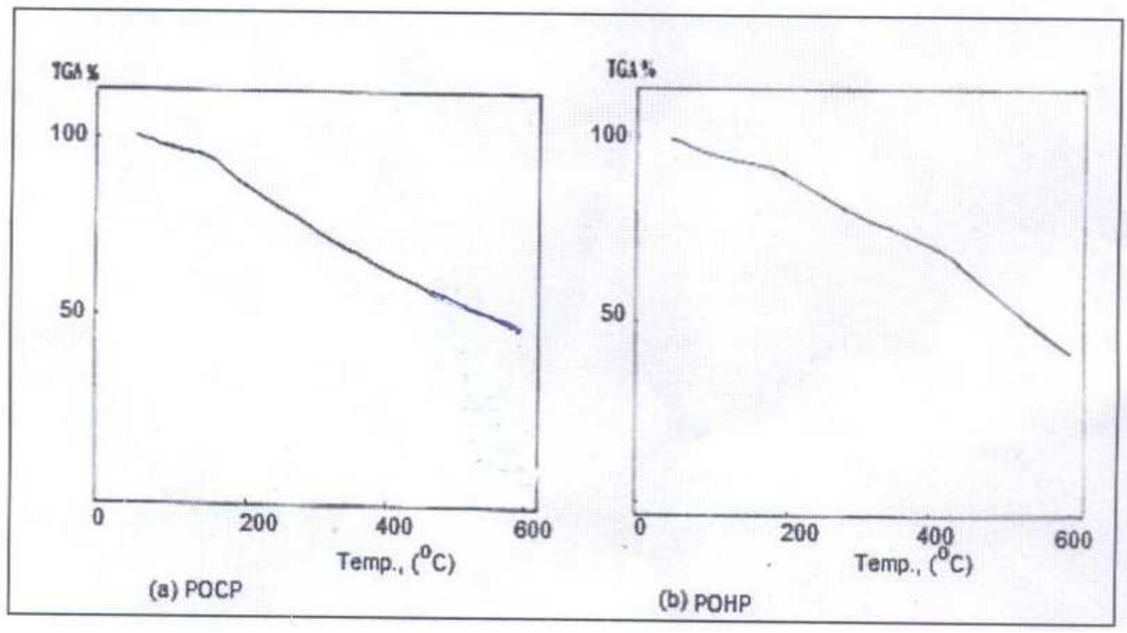

Fig. 13. TGA of POCP and POHP.

The second stage: includes the loss of the dopant species , SO_3 and one OH-radical and H_2O of sulfuric acid in the temperature range between 100 °C and 250 °C , the weight loss for this step was found to be(14.68%) which is in good agreement with the calculated value (14.7%)

The third stage: in the temperature range between 250 °C and 400 °C, includes the benzenoid ring and 5 molecules of OH-.The weight loss for this step was found to be (24.8 %) which is in good agreement with the calculated value(24. 6%).

The fourth step: the remaining part of the polymer decomposition,was found to be 56.17 in the range 400-600 °C and the calculated value is equal to 56.1. c.f. Table 6

Temperature range	Polymer name		The released molecules or Radicals
	POCLP	POHP	
	Calculated / found %	Calculated/ found %	
25-125	5.70 / 5.30	4.60 / 4.35	Two water molecule
100-250	--------	14.70 / 14.68	SO_3+H_2O+hydroxyl radical
120-400	24.80 / 24.04	-------	SO_3+ one molecule of benzenoide
250-400	--------	24.60 / 24.80	One molecule of benzenoide + 5hydroxyl radicals
400-600	69.50 / 70.66	56.10 / 65.17	The remained polymeric chain

Table 6. TGA analysis of POCP and POHP

3.4.2.5 Surface morphology study

In most conditions, a homogeneous, smooth and well-adhering brown POCP or black POHP films were electrodeposited on platinum electrode surfaces. The X-ray diffraction pattern shows that the prepared polymers are amorphous as shown in Figure 14 (a and b).

The surface morphology of the polymers obtained at the optimum conditions was examined by scanning electron microscopy. The SEM micrographs show a smooth lamellar surface feature of POCP and a smooth feature with uniform thickness for POHP (c.f., Fig 14 (c and d)).

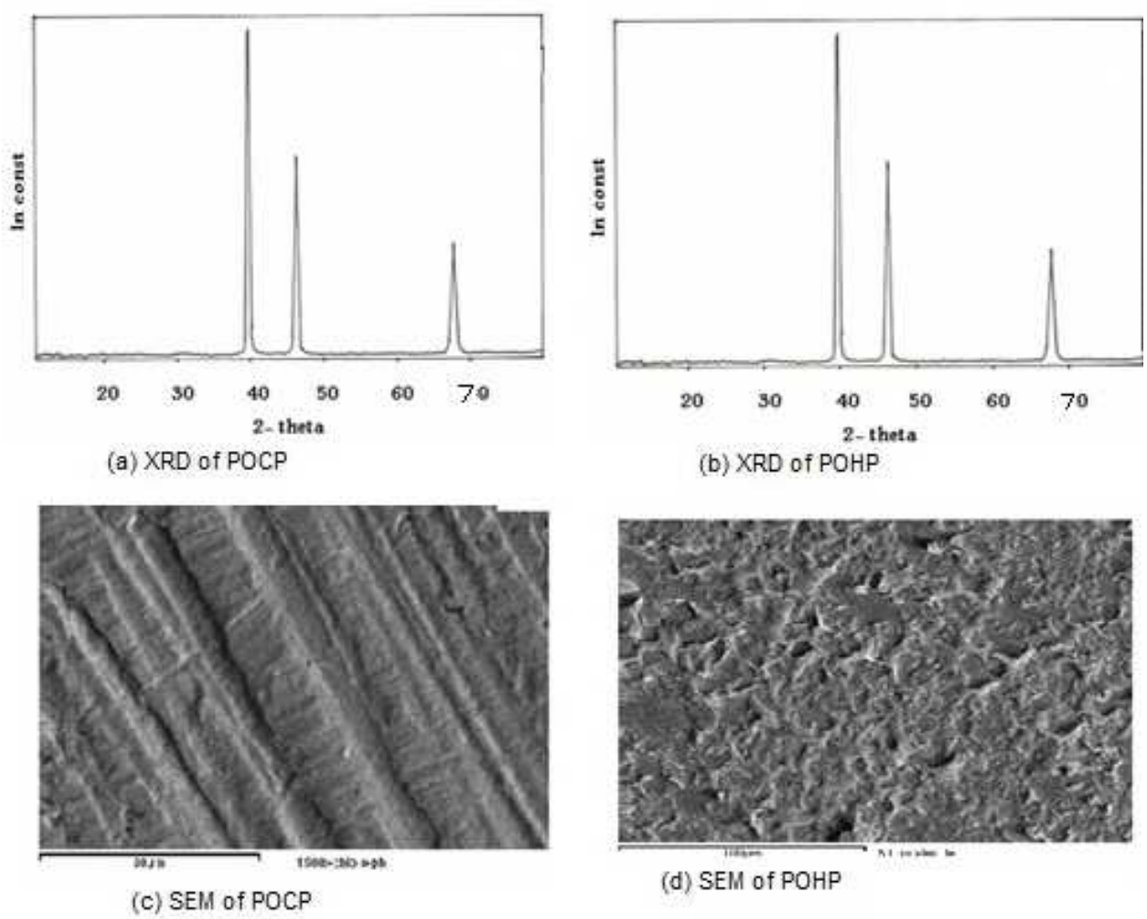

Fig. 14. XRD and SEM of POCP and POHP adhere Pt surfaces.

3.5 Application of the polyphenols as a pH sensor and dye removal.

3.5.1 The pH sensors

Hydrogen ion is ubiquitous species encountered in most chemical reactions. It quantified in terms of pH –the negative logarithm of its activity:

$$pH = - \log [H] \quad (5)$$

The pH sensors are widely used in chemical and biological applications such as environmental monitoring (water quality), blood pH measurements and laboratory pH measurements amongst others. The earliest method of pH measurement was by means of chemical indicators, e.g. litmus paper that changes its colour in accordance to a solution's pH. For example, when litmus is added to a basic solution it turns blue, while when added to an acidic solution the produced colour is red. Since many chemical processes are based on pH, almost all aqua samples have their pH tested at some point. The most common systems for pH sensing are based upon either amperometric or potentiometric devices. The most popular potentiometric approach utilises a glass electrode because of its high selectivity for hydrogen ions in a solution, reliability and straight forward operation. Ion selective membranes, ion selective field effect transistors, two terminal microsensors, fibre optic and fluorescent sensor, metal oxide and conductometric pH-sensing devices have also been developed . However, these types of devices can often suffer from instability or drift and, therefore, require constant re-calibration. Although litmus indicators and other above-mentioned pH sensors are still widely used in numerous areas, considerable research interest is now focused on the development of chemical or biological sensors using functional polymers. Thus, electrosynthesized polymers are considered to be good candidates as pH sensors due to the fact that they are strongly bonded to the electrode surfaces during the Electropolymerization step.

3.5.1.1 POCP modified Pt- electrode as pH sensor

3.5.1.1.1 Potentiometric study of POCP

In recent years, there has been a growing interest in electropolymerized film chemically modified electrodes and their application as potentiometric sensor particularly as P^H sensor. To investigate the effect of the thickness on the potentiometric response. POCP modified electrode of different thickness were prepared. Fig. (15) shows the potentiometric response of POCP film electrode in a wide range of pH (2-11) as a function of thickness ,we observed that this electrode gave a linear response over pH range with potentiometric slope values ranging from 26.6 to 40.72 mV/pH with the difference of the thickness as summarized in Table (7).

	At pH range (2-12)		At pH range (5-9)	
No of Cycles	-slope, (mV/pH)	r^2	-slope, (mV/pH)	r^2
3	40.72	0.96	56.19	0.98
5	37.70	0.99	42.12	0.98
10	31.70	0.96	35.09	0.99
15	26.60	0.93	28.11	0.85

Table 7. the potentiometric response of POCP modified electrode with different thickness at different range of pH.

From Figure 15 and Table 7, it is clear that the calculated potentiometric slope decreased as the polymer film thickness increased. Where the thin film of POCP electrode shows potentiometric slope equal to 40.7mV/pH and the thickest POCP shows decrease in potentiometric slope equal to 26.60 mV/pH, this decrease may be attributed to the diffusion rate of hydrogen ion across this modified electrode.

But when we use more limited pH range (4-9) as shown in Fig. 16 we noticed that the potentiometric response improved where the potentiometric slope was found to be 56.19 mV/pH for the thin POCP and decreased to 28.11 mV/pH for the thickest POCP film, from this result we noticed that this electrode might not an effective pH sensor for more basic or more acidic solutions but it is a good sensor in moderate pH range.

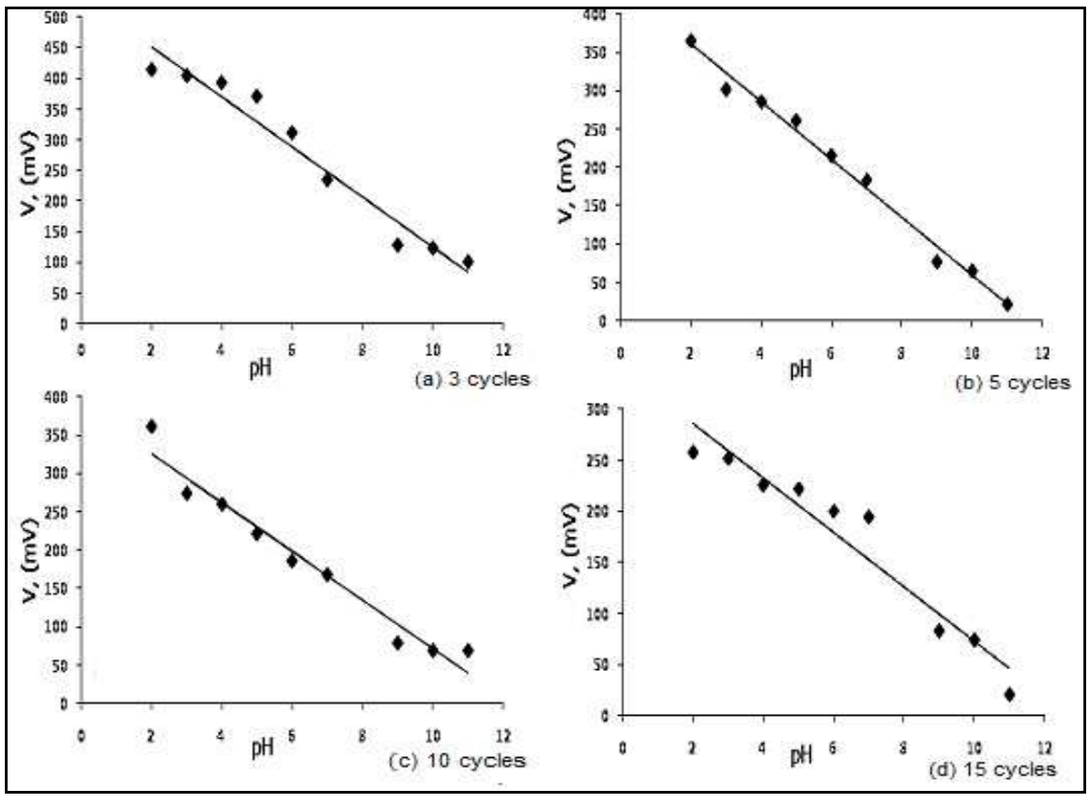

Fig. 15. POCP response at different pH values (2-12), the prepared film after different no of cycles.

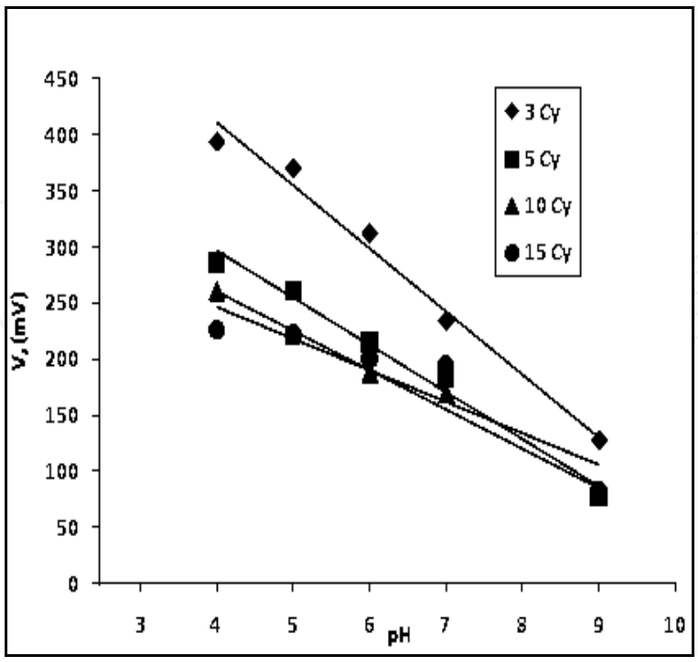

Fig. 16. POCP response at pH range (4-9) with different thicknesses

3.5.1.1.2 Electrode stability

The Potentiometric response of the chemically modified POCP electrode was examined over a period of 9 days in order to test the stability of the electrode. We observed that the chemically modified electrode shows linear behavior from pH (4-10) during 9 days as shown from Table 8 and Fig. 17 and the sensitivity of this coating decrease considerably with time since the slope varies from 40.7 at the first day to25.5mV/pH unit at the ninth day. Consequently polymer coating is not stable over a period of 9 days and the sensor cannot be used for several measurements. However, this electrode can be sensitive for one use sensor due to its sensitivity during the first measurement. It is important to note that the POCP film was found to peel off the supported electrode and it is a possible reason for the change of response slope.

Time, (day)	-slope, (mV/pH)	r^2
1	42.66	0.97
2	34.71	0.94
3	29.2	0.94
4	27.46	0.87
5	24.46	0.89
6	24.51	0.93
7	29.23	0.92
8	31.60	0.90
9	24.51	0.93

Table 8. The slope and r^2 values of POCP at different time intervals.

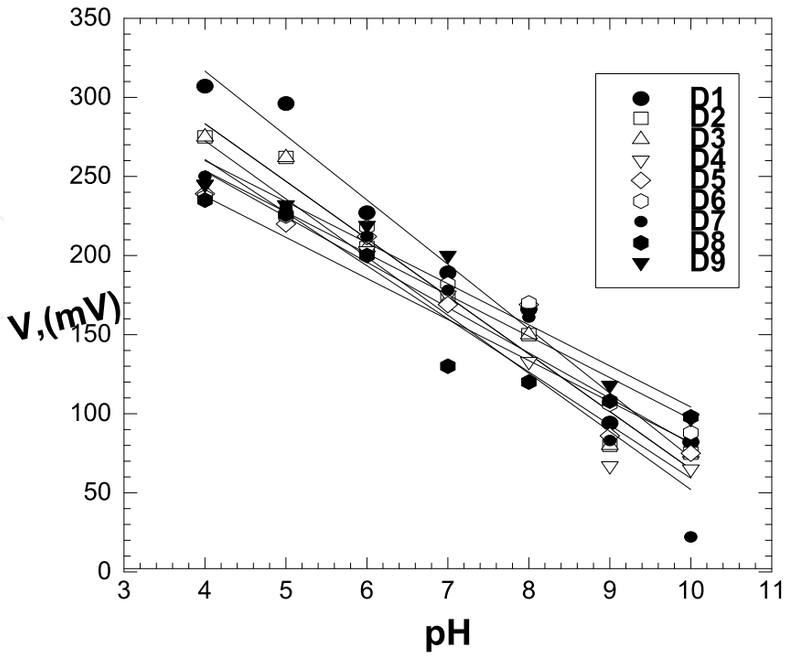

Fig. 17. P OCP response at different days, the prepared film from the first day to the ninth day

3.5.1.1.3 Response mechanism

We have shown that the potentiometric responses to pH changes of the different modified electrodes are linear in the range 4–9. These responses must be mainly attributed to the polymer films rather than the platinum substrate. Possible explanation is the affinity of the numerous hydroxyl groups and Cl atoms to the protons in solutions. The reaction of H^+ onto polymer creates local charge density excess at the electrode surface. Surface reactions seem to take place on the polymer film, essentially protonation and deprotonation of superficial OH groups of the polymers as symbolically described as follow;

$$P\ (\text{Polymer}) + H^+ \longrightarrow PH^+ \tag{6}$$

When the equilibrium is reached at the polymer/solution interface, we can write the equilibrium expression K of the surface reaction (1) and the equilibrium potential E as:

$$K = \frac{[PH^+]}{([P][H^+])} \tag{7}$$

and

$$E = E_0 + \left(\frac{RT}{F}\right)\ln\left(\frac{[PH^+]}{[P]}\right) = E_0' + \left(\frac{RT}{F}\right)\ln[H^+] \tag{8}$$

According to this mechanism of reaction, we are waiting for a potentiometric response slope of 59 mV/pH unit at 25 °C at all pH values. But our electrodes showed lower response slope. The presence of anionic and cationic responses of the polymer film electrodes, due to

the presence of ions (K^+, Na^+, Cl^-,….etc of the buffer solutions) in the different solutions probably caused this difference of response slope.

3.5.2 Dye removal

Water resources are of critical importance to both natural ecosystem and human developments. Increasing environmental pollution from industrial wastewater particularly in developing countries is of major concern. Many industries like dye industries, textile, paper and plastics, use dyes in order to color their products. As a result they generate a considerable amount of colored wastewater. The presence of small amount of dyes (less than 1 ppm) is highly visible and undesirable. Many of these dyes are also toxic and even carcinogenic and pose a serious threat to living organisms. Hence, there is a need to treat wastewaters containing toxic dyes and metals before they are discharged into the water bodies.

Many different treatment methods, including biological treatment, coagulation/flocculation, ozone treatment, chemical oxidation, membrane filtration, ion exchange, photocatalytic degradation and adsorption have been developed for the removal of dyes from wastewaters to decrease their impact in environment. Among these methods, adsorption is a well known separation process and is widely used to remove certain classes of chemical pollutants from waters, especially those that are practically unaffected by conventional biological treatments.

3.5.2.1 POHP as MB dye adsorbent

3.5.2.1 Adsorption kinetics

The adsorption kinetics was conducted to determine the optimum adsorption time for the adsorption of MB dye by POHP. The effect of the contact time on adsorption of MB onto POHP is represented in Fig. 18.

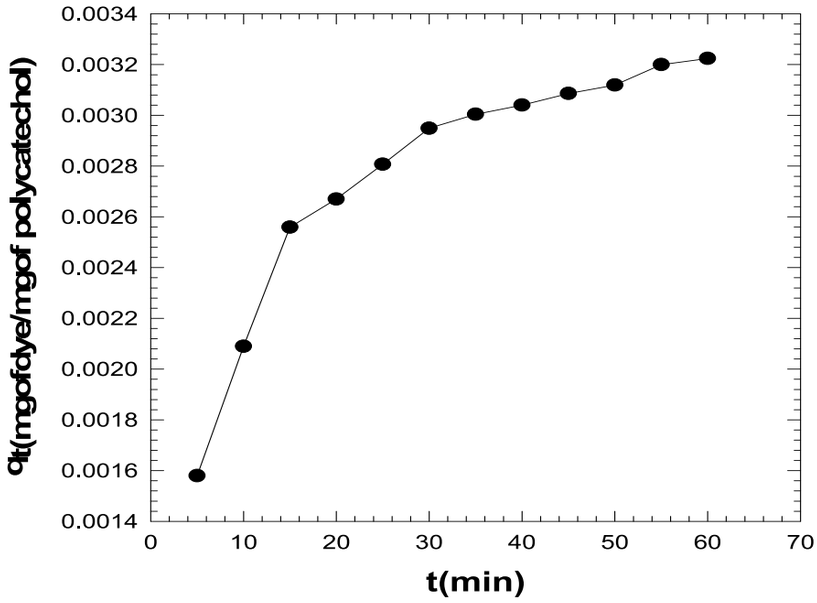

Fig. 18. The effect of contact time on adsorption of MB onto POHP.

The adsorption capacity increases rapidly during the initial adsorption stage and then continues to increase at a relatively slow speed with contact time. The obtained result reveals that, at the beginning, the adsorption mainly occurs on the surface of POHP so the adsorption rate is fast. After the surface adsorption is saturated, the adsorption gradually proceeds into the inner part of POHP via the diffusion of MB dye into the polymer matrix, leading to a lower adsorption rate In order to evaluate the adsorption kinetics of MB dye onto POHP, the pseudo-first-order, pseudo-second-order, intraparticle diffusion and Elovich models were employed to interpret the experimental data, as shown below:
Pseudo-first-order equation:

$$\text{Log } (q_e - q_t) = \log q_e - k_1 t/2. \quad (9)$$

Pseudo-second-order equation:

$$t/q_t = 1/k_2 q^2 e + t/ \quad (10)$$

Intraparticle diffusion equation:

$$q_t = k i t^{0.5} + \quad (11)$$

Elovich equation:

$$q_t = b + a \ln \quad (12)$$

Where q_e and q_t are the amounts of dye adsorbed (mg mg^{-1}) at equilibrium and at time t (min), and t is the adsorption time (min). The other parameters are different kinetics constants, which can be determined by regression of the experimental data. The validities of these four kinetic models are checked and graphically represented in Fig. 19. The corresponding kinetic parameters and the correlation coefficients are summarized in Table 9. Based on linear regression (r^2) values, the adsorption kinetics of MB dye have the following order. pseudo-second order > Elovich > pseudo-first-order > intraparticle diffusion models.

Kinetic models	Parameters		r^2
Pseudo-first-order	k_1(min^{-1}) q_e, (mg mg^{-1})	0.02303 1.81×10^{-3}	0.934
Pseudo-second-order	k_2 (mg mg^{-1} min^{-1}) q_e, cal (mg mg−1)	40.32 0.0036	0.999
Intraparticle diffusion	K_i(mg $mg^{-1}min^{-0.5}$) C(mg mg^{-1})	2.68×10^{-4} 1.31×10-3	0.891
Elovich	a b	6.46×10^{-4} 6.59×10^{-4}	0.972

Table 9. Kinetic parameters for adsorption of MB onto POHP.

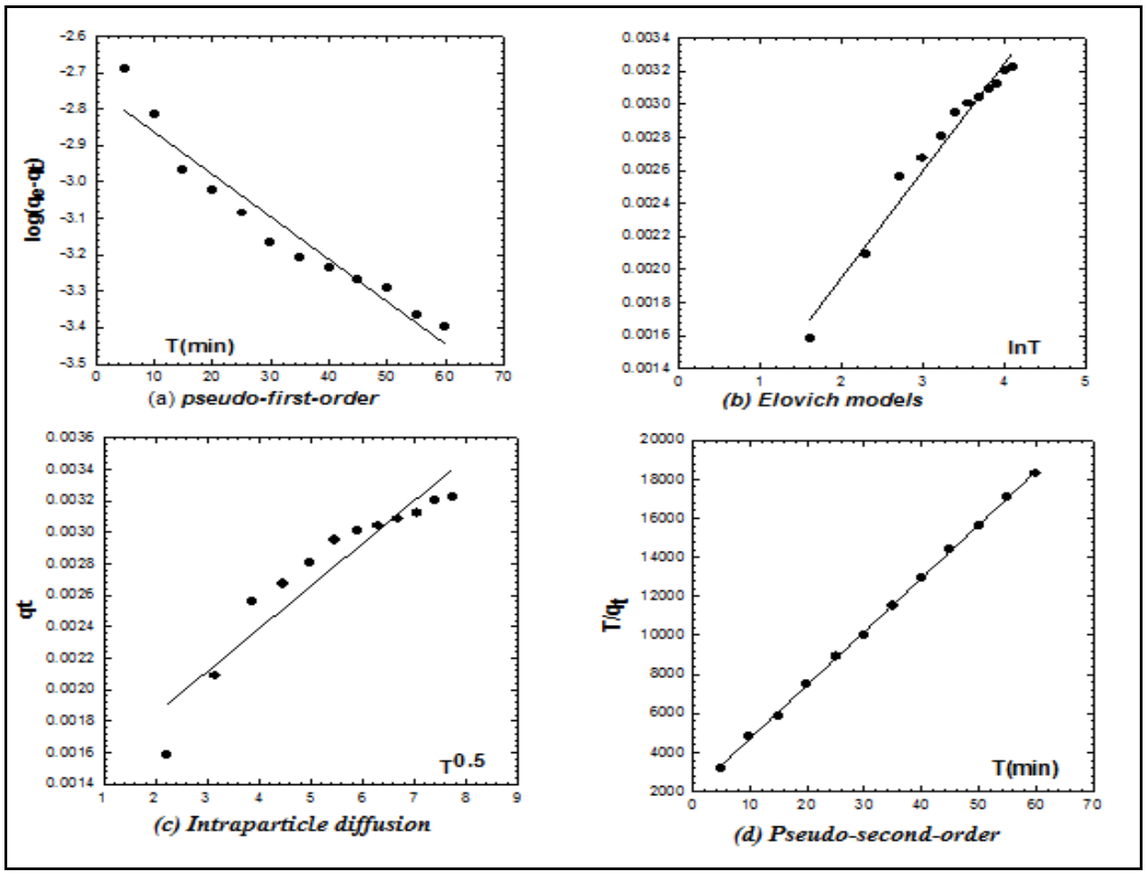

Fig. 19. Adsorption kinetics of MB dye onto POHP.

3.5.2.2 Adsorption isotherm

The adsorption isotherm of MB dye onto POHP is represented in Fig 20. The adsorption capacity of MB dye increases with the increase of dye concentration. This may be attributed to the extent of a driving force of concentration gradients with the increase of dye concentration. Then tends to level off, this is due to the saturation of the sorption site on the adsorbent.

3.5.2.3 Equilibrium isotherm models

The adsorption isotherm is fundamental in describing the specific relation between the concentration of adsorbate and the adsorption capacity of an adsorbent, and it is important for the design of adsorption system. In this study, two important isotherms are selected, that is, Langmuir and Freundlich models, to describe the experimental results of MB dye adsorption on POHP are summarized in Table 10.

The Langmuir isotherm assumes that the adsorption occurs at specific homogeneous sites on the adsorbent and is the most commonly used model for monolayer adsorption process, as represented by Fig. 21 and the following equation:

$$C_e/\ q_e\ = 1/bqm + C_e/\ gm \tag{13}$$

Where the constant b is related to the energy of adsorption (Lmg^{-1}), and q_m is the Langmuir monomolecular adsorption capacity ($mg\ mg^{-1}$).

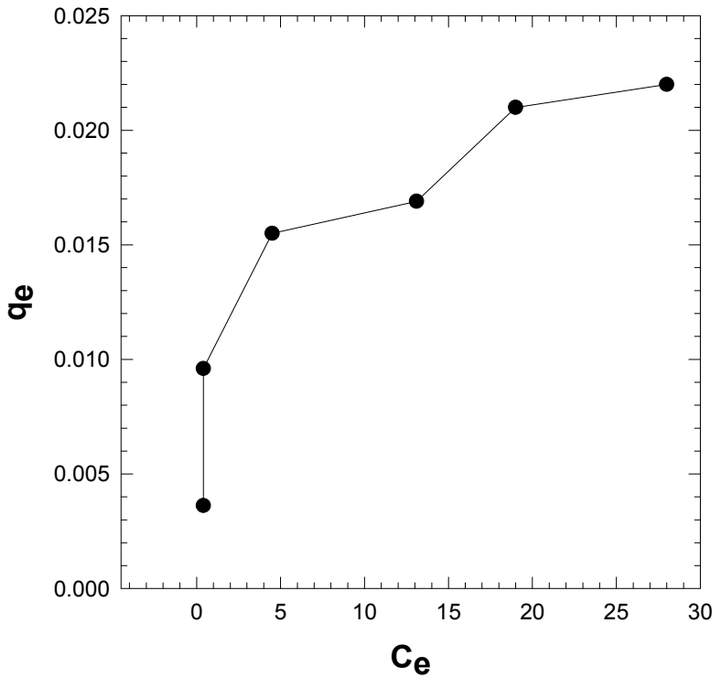

Fig. 20. Adsorption isotherms of MB onto POHP

The essential characteristics of the Langmuir isotherm can be expressed in terms of a dimensionless constant separation factor R_L represented by the equation .

$$R_L = 1/(1 + bC_o) \quad (14)$$

where C_o (mg L^{-1}) is the initial dye concentration. If the value of R_L lies between 0 and 1, the adsorption is favorable.

The Freundlich isotherm is an empirical equation assuming that the adsorption process takes place on heterogeneous surfaces and adsorption capacity is related to the concentration of dye at equilibrium is described by Fig. (21) and the following equation:

$$\log q_e = \log K_f + 1/n \log C_e \quad (15)$$

where K_f (mg mg^{-1}) is roughly an indicator of the adsorption capacity and 1/n is the adsorption intensity.

Sample	Langmiur				Freundlich		
POHP	q_m	b	R_L	r^2	n	Ln K_f	r^2
	0.023	0.34	0.42	0.99	1.74	5.16	0.972

Table 10. Langmiur and freundlich isotherm constants of the adsorption of MB dye on POHP.

It is shown that the applicability of the above adsorption isotherms was compared by judging the correlation coefficients. The results indicate that the Langmuir isotherm fits quite well with the experimental data (r^2= 0.99), whereas, the low correlation coefficients (r^2 > 0.97) show the poor agreements of the Freundlich isotherm with the experimental data. The value of n for Freundlich isotherm is greater than 1, mean while the values of R_L lie between 0 and 1, indicating that MB dye is favorably adsorbed by POHP.

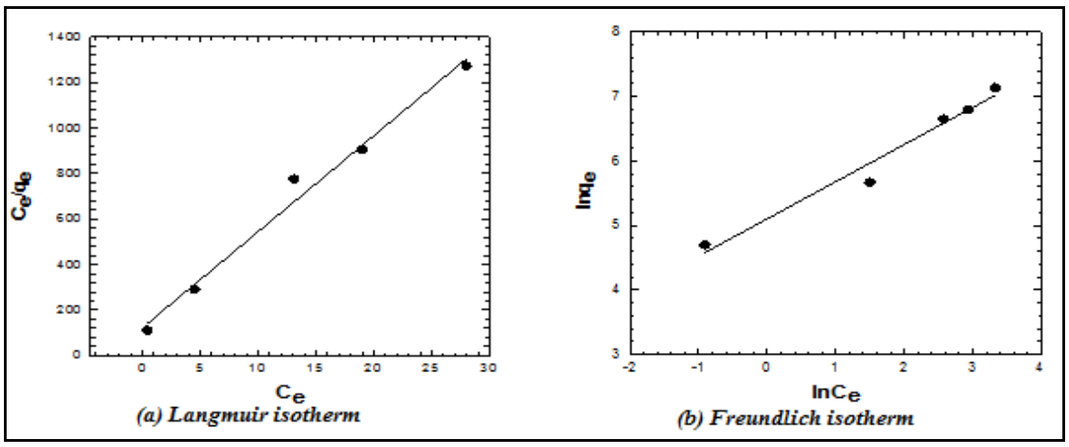

Fig. 21. Langmiur and Frendlich isotherms for adsorption of MB dye on POHP.

4. Conclusions

Cv is useful tool in oxidation of pollutants as phenols. The electropolymerization, by cyclic voltammetry, of phenols on Pt-surfaces is a notoriously complex process which depends on the phenols structure, the potential scan rate, the pH, the temperature and the phenols concentration. Comparing the voltammograms from the different monomer compound solutions, it was demonstrated that the polymer film resulting from both OCP and OHP oxidation leads to the higher surface deactivation degree. This is probably due to the higher adhering properties of POCP and POHP to Pt-surface.

The proposed mechanisms are well confirmed by different tools and agree with that mentioned in literatures.

The oxidation processes are partially controlled processes with stable diffusion coefficients at different scan rates.

The Obtained polymers are amorphous with higher thermal stability with smooth lamellar surface feature for POCP and a smooth feature with uniform thickness for POHP.

POCP modified Pt electrode could be used as one use pH sensor with good response and perfect Nernstian- slope especially at pH range 4-9 but its poor pH sensor at more acidic or basic solution and loose its response by time.

More work must be done to improve both response and stability of the sensor.

POHP is a perfect adsorbent to MB dye from aqueous solution and must be used in purification of waste water.

5. Nomenclatures

CV	Cyclic Voltammetry
OCP	Ortho-chlorophenol

OHP	Ortho Hydroxyphenol
POCP	Poly orthochlorophenol
POHP	Poly orthohydroxy phenol
MB	Methelene blue dye
TGA	Thermal gravemetric analysis
XRD	X-ray diffraction analysis
SEM	Scaninng electron microscopy
UV-vis.	UV-visible spectroscopy
IR	Infra red spectroscopy
^{1}HNMR	Nuclear Magnetic Resonance Spectroscopy
WE	Working electrode
SB	Salt bridge
CE	Counter Electrode
SCE	Saturated Calomel electrode

6. References

Ardakani, M.M., Sadeghiane, A., Moosavizadeh, S., Karimi, M. A., Mashhadizadeh, M. H.(2009). Electrocatalytic Determination of Hydrazine using Glassy Carbon Electrode with Calmagates, Anal. Bioanal. Electrochem. 1(3) : 224-338.

Arslan, G.; Yazici, B & Erbil, M. (2005) . The effect of pH, temperature and concentration on electrooxidation of phenol, Journal of Hazardous Materials B124: 37–43

Comninellis, C. (1994). Electrocatalysis in the electrochemical conversion/combustion of organic pollutants for waste water treatment, Electrochimica Acta, 39 (11-12): 1857-1862.

Ezerskis Z., & Jusys, Z. (2002). Electropolymerization of chlorinated phenols on a Pt electrode in alkaline solution. Part IV: A gas chromatography mass spectrometry study, Journal of Applied Electrochemistry, 32 (5): 543-550.

Fleszar, B. & Jolanta, P. (1985), An attempt to define benzene and phenol electrochemical oxidation mechanism, Electrochimica Acta, 30 (1) : 31-42.

Gattrell, M., & Kirk, D.W.(1993). Study of electrode passivation during aqueous phenol electrolysis, Journal of the Electrochemical Society, 140(4) : 903-911

Gutiérrez, C. (2002).Electrooxidation of 2,4-dichlorophenol and other polychlorinated phenols at a glassy carbon electrode, Electrochim. Acta, 47(15): 2399. Iotov, P.I.& Kalcheva, S.V. (1998). Mechanistic approach to the oxidation of phenol at a platinum/gold electrode in an acid medium , Journal of Electroanalytical Chemistry, 442(1-2) : 19-26. Randles, J. E. B.(1948). A cathode ray polarograph. II. The current voltage curves, Trans. Faraday Soc, 44 : 327-338.

Sayyah, S. M., Abd El-Rehim, S. S., El-Deeb, M. M., Kamal, S. M. & Azooz, R. E., (2010). Electropolymerization of p- Phenylenediamine on Pt-Electrode from Aqueous Acidic Solution: Kinetics, Mechanism, Electrochemical Studies, and Characterization of the Polymer Obtained, J Appl Polym Sci 117: 943–952

Sevick, A. (1948), Oscillographic polarography with periodical triangular voltage, Collect. Czech. Chem. Commun., 13 349-377.

Wang, J., Jiang, M. & Lu, F. (1998), Electrochemical quartz crystal microbalance investigation of surface fouling due to phenol oxidation, Journal of Electroanalytical Chemistry, 444(1, 5) : 127-132

Wang, J., Martinez, T. Daphna, Y. R. & McCormick, L.D. (1991). Scanning tunneling microscopic investigation of surface fouling of glassy carbon surfaces due to phenol oxidation, Journal of Electroanalytical Chemistry and Interfacial Electrochemistry, 313 (1-2): 129-140

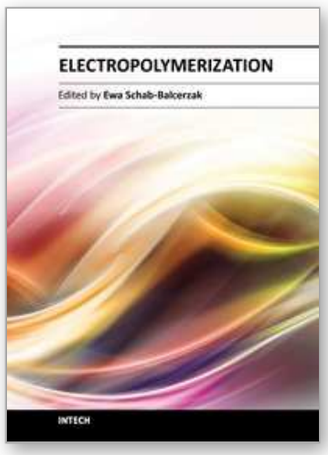

Electropolymerization

Edited by Dr. Ewa Schab-Balcerzak

ISBN 978-953-307-693-5
Hard cover, 214 pages
Publisher InTech
Published online 22, December, 2011
Published in print edition December, 2011

In recent years, great focus has been placed upon polymer thin films. These polymer thin films are important in many technological applications, ranging from coatings and adhesives to organic electronic devices, including sensors and detectors. Electrochemical polymerization is preferable, especially if the polymeric product is intended for use as polymer thin films, because electrogeneration allows fine control over the film thickness, an important parameter for fabrication of devices. Moreover, it was demonstrated that it is possible to modify the material properties by parameter control of the electrodeposition process. Electrochemistry is an excellent tool, not only for synthesis, but also for characterization and application of various types of materials. This book provides a timely overview of a current state of knowledge regarding the use of electropolymerization for new materials preparation, including conducting polymers and various possibilities of applications.

How to reference

In order to correctly reference this scholarly work, feel free to copy and paste the following:

S.M. Sayyah, A.B. Khaliel, R.E. Azooz and F. Mohamed (2011). Electropolymerization of Some Ortho-Substituted Phenol Derivatives on Pt-Electrode from Aqueous Acidic Solution; Kinetics, Mechanism, Electrochemical Studies and Characterization of the Polymer Obtained, Electropolymerization, Dr. Ewa Schab-Balcerzak (Ed.), ISBN: 978-953-307-693-5, InTech, Available from: http://www.intechopen.com/books/electropolymerization/electropolymerization-of-some-ortho-substituted-phenol-derivatives-on-pt-electrode-from-aqueous-acid

INTECH
open science | open minds

InTech Europe
University Campus STeP Ri
Slavka Krautzeka 83/A
51000 Rijeka, Croatia
Phone: +385 (51) 770 447
Fax: +385 (51) 686 166
www.intechopen.com

InTech China
Unit 405, Office Block, Hotel Equatorial Shanghai
No.65, Yan An Road (West), Shanghai, 200040, China
中国上海市延安西路65号上海国际贵都大饭店办公楼405单元
Phone: +86-21-62489820
Fax: +86-21-62489821

IntechOpen